POLITECNICO DI TORINO

Corso di Laurea Magistrale in Ingegneria Biomedica

Master thesis in Biomedical engineering

Evaluation of mechanical properties of multiscale engineered tissues and optimization of single cell encapsulation methods

Internal supervisor: Prof. Chiara Tonda-Turo
External supervisor: Dr. Jeroen C.H. Leijten
Candidate: Matteo Genitrini, 224885

Table of the contents

Chapter 1

1.1 Cartilage properties

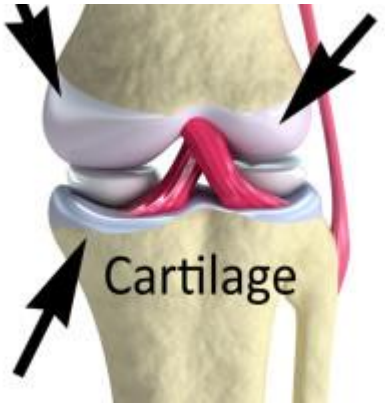

Figure 1 Cartilage at knee joint

Cartilage is a very resilient, load bearing and important tissue in human body. Its main task consists of covering the bone ends in proximity of the joints (figure 1), in order to protect the bone itself and allow the joints to move easily, minimizing friction and without pain. It can tolerate mechanical stress without permanent distortion. Also, it is not as hard and rigid as bone, but much stiffer and less flexible than muscle.

In humans it can be found, as already mentioned, at the end of long bones, but also in ears, in nose, bronchial tubes, intervertebral discs and many other sites (figure 2).
Because of its rigidity, cartilage often fullfills the purpose of holding tubes open in the body (e.g. the rings of trachea).

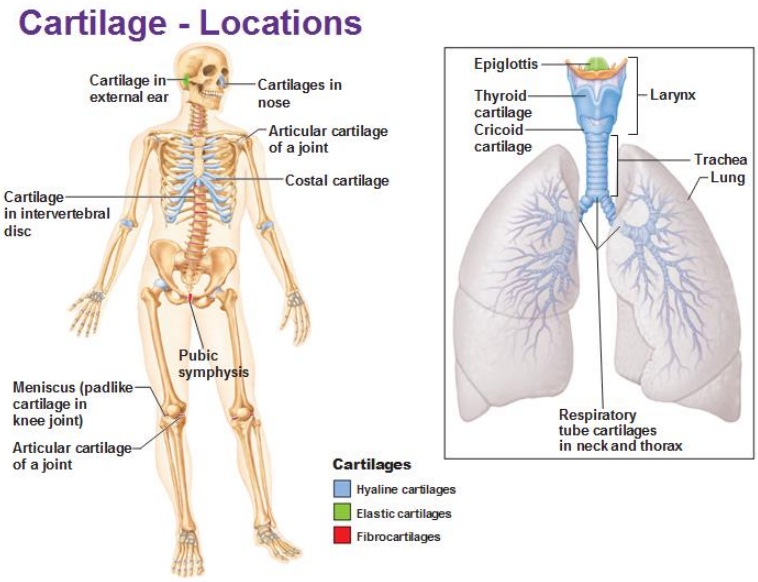

Figure 2 Cartilage locations in human body

1.2 Cartilage histology

There exist three different types of cartilage: elastic cartilage, hyaline caritlage and fibrous cartilage.

1.2.1 Hyaline cartilage

Hyaline is a glass like but translucent tissue. It is possible to find it in many joint surfaces (this is why it is also called articular cartilage), and it is the most abundant type of cartilage in human body.The thickness is 2 to 4mm [1].

Articular cartilage is made up by specialized cells called chondrocytes, wich are the only cell type found in normal articular cartilage, and are mesenchymal in origin [2]. Chondrocytes contribute to less than 2% of the wet weight in healthy adult tissue [3]. They produce a large amount of collagenous extra cellular matrix (ECM). Such cells, under nonpathological conditions, have a spheroid morphology, 10–20 µm in diameter and relatively distant from each other. They are housed in lacunae, which are small cavities that surround the cells [4].
As in cartilage nerves and blood vessels are absent, nutrition is supplied to chondrocytes by diffusion from capillaries in adjacent connective tissue (perichondrium). Compared to other connective tissues, cartilage has a very slow turnover of its extracellular matrix and does not repair.

It is externally covered by a fibrous membrane called perichondrium which provides nutrients to the cartilage since, as already mentioned, the cartilage tissue has no blood vessels of its own. Articular cartilage structure consists of four adjacent, interdigitating and organized zones. These are, from the tissue exposed to the synovial fluid in the direction of the subchondral bone, the superficial-, middle-, deep- and calcified zone (figure 3-4).

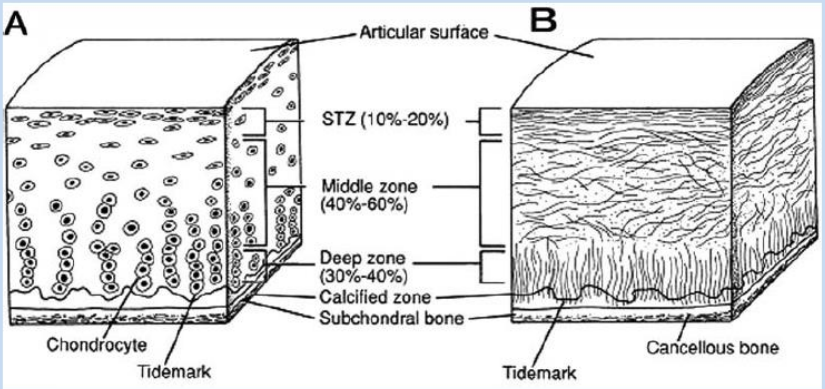

Figure 2. Schematic, cross-sectional diagram of healthy articular cartilage: A, cellular organization in the zones of articular cartilage; B, collagen fiber architecture. (Copyright American Academy of Orthopaedic Surgeons. Reprinted from the *Journal of the American Academy of Orthopaedic Surgeons*, 1994;2:192-201 with permission.[11])

Figure 3 Hyaline cartilage schematic illustration

- The thin superficial (tangential) zone [1] protects deeper layers from shear stresses and makes up approximately 10% to 20% of articular cartilage thickness. The collagen fibers of this zone (primarily, type II and IX collagen) are packed tightly and aligned parallel to the articular surface. The superficial layer contains a relatively high number of flattened chondrocytes, and the integrity of this layer is imperative in the protection and maintenance of deeper layers. This zone is in contact with synovial fluid and is responsible for most of the tensile properties of cartilage, which enable it to resist the sheer, tensile, and compressive forces imposed by articulation.

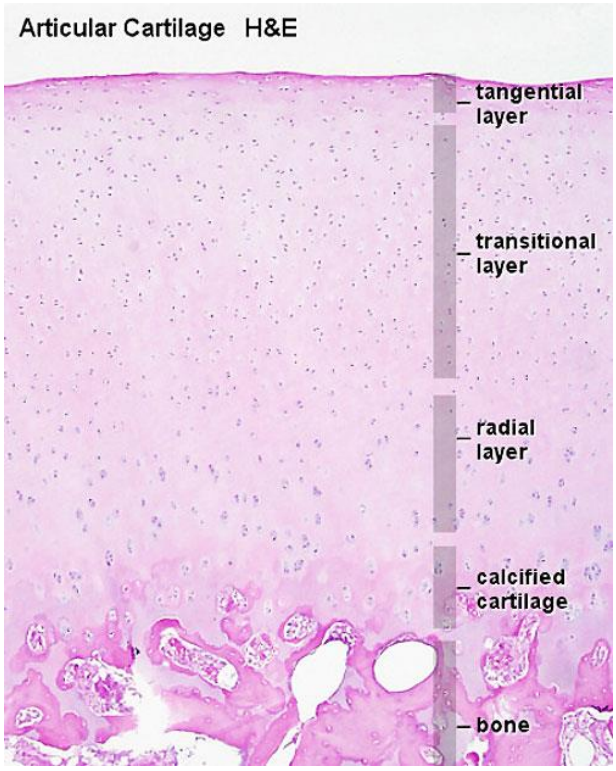

Figure 4 Hyaline cartilage histology

- Immediately deep to the superficial zone is the middle (transitional) zone [1], which provides an anatomic and functional bridge between the superficial and deep zones. The middle zone represents 40% to 60% of the total cartilage volume, and it contains proteoglycans and thicker collagen fibrils. In this layer, the collagen is organized obliquely, and the chondrocytes are spherical and at low density. Functionally, the middle zone is the first line of resistance to compressive forces.

- The deep zone [1] is responsible for providing the greatest resistance to compressive forces, given that collagen fibrils are arranged perpendicular to the articular surface. The deep zone contains the largest diameter collagen fibrils in a radial disposition, the highest proteoglycan content, and the lowest water concentration.

- The calcified layer [1] plays an integral role in securing the cartilage to bone, by anchoring the collagen fibrils of the deep zone to subchondral bone. In this zone, the cell population is scarce and chondrocytes are hypertrophic.

As far as in concerns composition (figure5), articular cartilage is highly hydrated and consisting approximately of:

- 70% of water
- 30% of ECM
  - 60% of collagen (mainly type II)
  - 25-35% of proteoglycans (aggrecans)
  - 15-20% of noncollagenous proteins and glycoproteins.

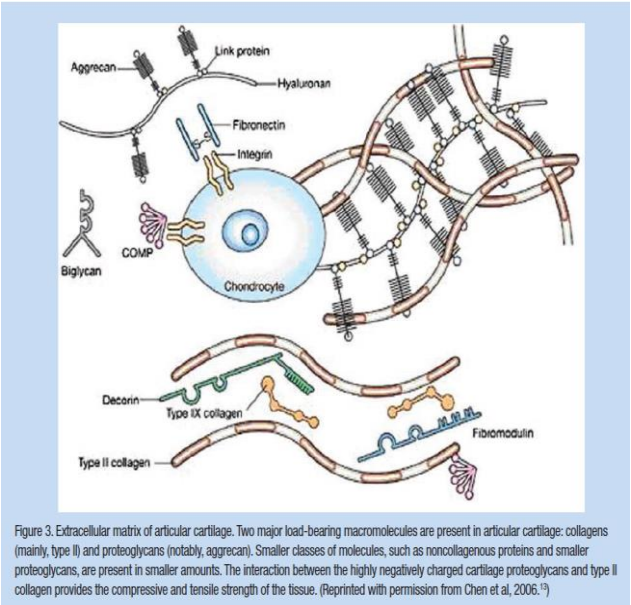

Figure 3. Extracellular matrix of articular cartilage. Two major load-bearing macromolecules are present in articular cartilage: collagens (mainly, type II) and proteoglycans (notably, aggrecan). Smaller classes of molecules, such as noncollagenous proteins and smaller proteoglycans, are present in smaller amounts. The interaction between the highly negatively charged cartilage proteoglycans and type II collagen provides the compressive and tensile strength of the tissue. (Reprinted with permission from Chen et al, 2006.[13])

Figure 5 ECM composition

In close association with bone, articular cartilage insures joint lubrication and movement. The GAG side chains of aggrecan are able to bind water molecules, thereby sequestering water and generating an internal swelling pressure within the cartilage matrix.

1.2.2 Elastic cartilage

Figure 6 Elastic cartilage representation

Fresh elastic cartilage appears more opaque and yellow than hyaline cartilage because of abundant elastic fibers in its matrix (figure 6). Elastic cartilage is resilient, easily returning to its original shape after bending or distortion, and has more flexibility and elasticity than other cartilage types. Its matrix contains a dense, interwoven network of elastic fibers embedded in a small amount of amorphous extracellular ground substance. This network is denser in the interior than at periphery. The spherical chondrocytes, which sit in lacunae, appear similar to chondrocytes of hyaline cartilage, except that they are more closely packed and and often found singly in the lacunae (only a few isogenous nets are present). The matrix also contains a small number of type II collagen fibers that are masked by ground substance

and intermingle with the more abundant elastic fibers. Like hyaline cartilage (other than that on articular surfaces of joints), elastic cartilage is envolved by a perichondrium. Blood vessels are lymphatics in the phericondrium do not penetrate the cartilage interior. Elastic cartilage undergoes either appositional growth, from the perichondrium, or interstitial growth, by chondrocyte mitosis. Elastic cartilage does not calcify with age [5]

1.2.3 Fibrocartilage

Fibrocartilage is found in the pubis symphysis, the annulus fibrosus of intervertebral discs, menisci, and the temporomandibular joint.
It is a mixture between dense regular connective tissue (similar in many respects to tendon or ligament) and hyaline cartilage. It combine the tensime strenght, firmness and durability of tendon with resistange to compression of cartilage.
In contrast to other types of cartilage, fibrocartilage lacks a distinct perichondrium, which blends imperceptibly with surrounding connective tissue or hyaline cartilage. Its matrix is intensely eosinophilic because numerous collagen fibers are present. Arranged in parallel bundles, often in line with the direction of pull or stress applied, they give a characteristic fibrous appearence to the matrix, which is readily seen in routine histologic preparations. The matrix contains a minimal amount of amorphous ground substance, which is usually seen at boundaries of lacunae, where it is slightly basophilic or stains positively for periodic acid Schidd (PAS). Chondrocytes are thinly dispersed in the matrix and are arranged in short, parallel rows between collagen fiber bundles. In contrast to hyaline cartilage, with type II collagen in its matrix, fibrocartilage is composed of type I collagen. Fibrocartilage initially forms from dense connective tissue that is rich in fibroblasts, some of which differendiate into chondrocytes. Thus, a mixture of chondrocytes and fibroblasts is characteristic of mature fibrocartilage [5].

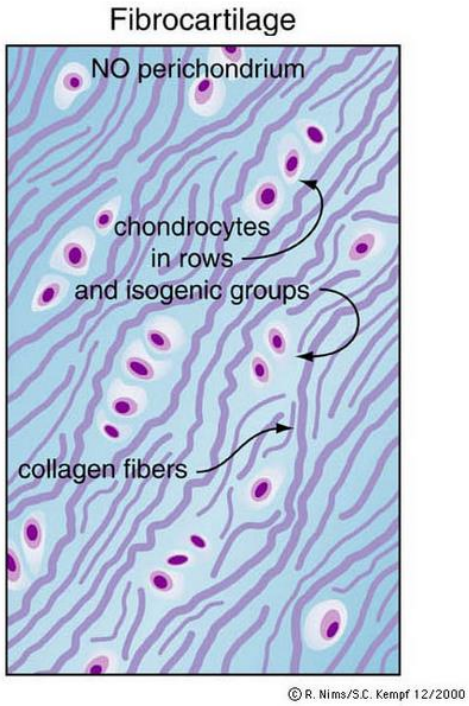

Figure 7 Fibrocartilage structure

1.3 Osteoarthritis

1.3.1 What is it

Osteoarthritis (OA), the most common musculoskeletal condition, is a long-term chronic disease involving the thinning of cartilage in joints which results in bones rubbing together, creating stiffness, pain, and impaired movement [6].
OA is related with age, but is associated with a variety of both modifiable and non-modifiable risk factors, including obesity, lack of exercise, genetic predisposition, bone density, occupational injury, trauma, and gender.

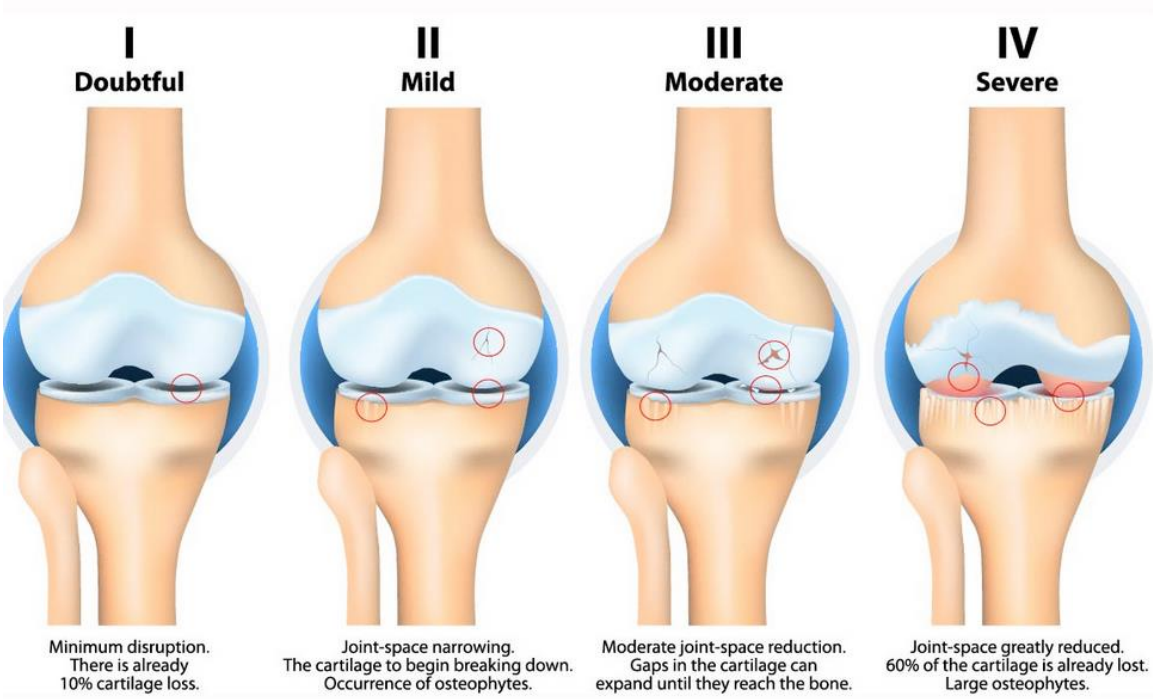

Figure 8 Osteoarthritis development

Osteoarthritis is characterized by the breakdown of cartilage in joints [7]. As cartilage deteriorates (figure 8), the bones of the joint begin to run against one another, causing stiffness and pain, which often impairs movement. Osteoarthritis also can damage ligaments, menisci, and muscles. Bone or cartilage fragments may float in the joint space, causing irritation and pain. Bone spurs, or osteophytes, may also develop, causing additional pain and potentially damaging surrounding tissues. Around the world, an estimated 10%-15% of adults over 60 have some degree of osteoarthritis.1 It most commonly affects the joints in the knee, hands, feet, and spine, and is also relatively common in other joints such as the shoulder and hip joints.
There are two types of osteoarthritis: primary and secondary.
Primary osteoarthritis is a chronic degenerative disease that is related to, but not caused by, aging. As a person ages, the water content of their cartilage decreases, thus weakening it and making it less resilient and more susceptible to degradation. There are strong indications that genetic inheritance is a factor, as up to 60% of all OA cases are thought to result from genetic factors [8].
Secondary arthritis tends to show up earlier in life, often due to a specific cause such as an injury, a job that requires kneeling or squatting for extended amounts of time, diabetes, or obesity. But

though the aetiology is different than that of primary OA, the resulting symptoms and pathology are the same.
The current control strategy mainly consists of palliative pain treatment, as there are several medicines on the market that alleviate pain and improve function in OA patients. In severe cases, joint replacement surgery has been proven effective in relieving the painful and debilitating effects of the disease, though the high cost and use of advanced resources mean these procedures are not available in many countries around the world.

1.3.2 Joint Replacement Surgery

The current control strategy mainly consists of palliative pain treatment, as there are several medicines on the market that alleviate pain and improve function in OA patients. In severe cases, joint replacement surgery has been proven effective in relieving the painful and debilitating effects of the disease, though the high cost and use of advanced resources mean these procedures are not available in many countries around the world.

The average age of a patient who receives a total hip replacement (THR, figure 9) in the United States is just under 68 years of age, and the likelihood of having the surgery increases with age [9].

Figure 9 Hip prosthesis

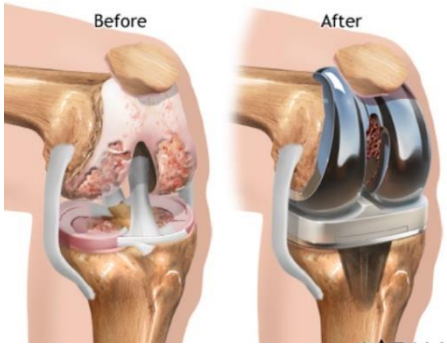

Figura 10 Knee prostheis

The same trend is apparent for total knee replacements (TKR, figure 10). The number of hip and knee replacement surgeries performed is projected to continue increasing at a rapid rate: between 2005 and 2030, hip arthroplasties are expected to increase by 174%, and the number of knee arthroplasties is expected to increase even more rapidly: increasing by 673% by 2030 [9. Though joint replacement surgeries are expensive procedures, their high effectiveness may justify their prevalence, especially in high-income countries that have adequate resources for such treatments.

1.4 Tissue engineering as an alternative

1.4.1Generalities

Nevertheless, the high cost of such type of surgery prevents lower-income countries, or people in general, from obtaining proper assistance.
In the last decades, a field that has been attracting even and even more the attenction of scientific comunity is tissue engineering, a science which consists of applying to biology and nanotechnology

the scientific principles and the strictness proper of engineering.
Specifically, tissue engineering (TE) aims to develop biological substitutes that restore,maintain or improve tissue functions [10] as a last step, to transplant the obtained tissues in the damaged site of patient's body (figure 11).

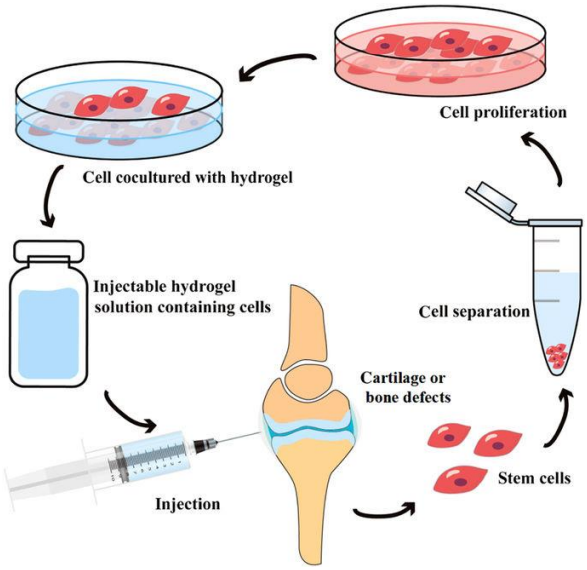

Figure 11 General TE folw chart

Briefly, after withdrawing cells from injured area through a biopsy, these are firstly isolated and then expanded throughout specific protocols. Afterwards, cells are encapsulated in specific biomaterials - preferably hydrogels- and then injected back into the patient; what we obtain is a scaffold as a temporary support matrix for cell growth, differentiation and matrix production

1.4.2 Why hydrogels

1.4.2.1 Hydrogels generalities

Hydrogel (three-dimensional polymeric networks) scaffolds, which have been widely investigated as candidates for cartilage TE, have high water content, providing an environment similar to physiological one (70% water! [4]). Furthermore this type of networks are able to allow a sufficient mass transportation, enabling to nutrients to reach cells and waste products to be carried out.
Biomimeticity is an essential prerequisite for the success of the implant, as well as biocompatibility biodegradability and mechanical strenght. When the scaffold is able to mimic the native environment, it is also able to support tissue-specific differentiation.
Degradation properties of hydrogels should be optimized to provide a good cell migration [11] and then a good ECM distribution [12-17] . Degradable hydrogels are generally derived from natural or synthetic degradable polymersor absorbable polymers. Typical examples are gels containing hyaluronic acid (HA), collagen, chitosan.
Degradations means loss of mechanical strenght, hence degradation rate should be comparable with the rate of tissue formation.

1.4.2.2 Crosslinking methods

Hydrogels can be classified into chemical and physical gels according to the type of crosslinking present in its network.

- Chemical crosslinking:

- Radical polymerization: vynil-bearing groups can be polymerized to form hydrogels using redox- or thermaly-initiated or photo- polymerization (figure 12). Commonly used macromers are PVA, PEG (syntethics), HA, chitosan, dextran.

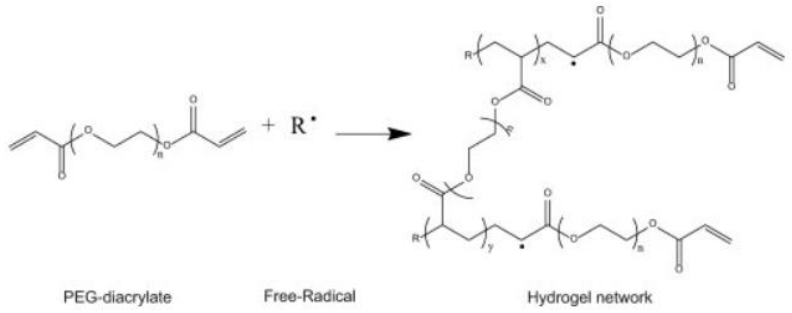

Figure 12 photopolymerization

- Crosslinking through functional groups: typical reactions are Shiff-base formation or Michael-type additions (figure 13).

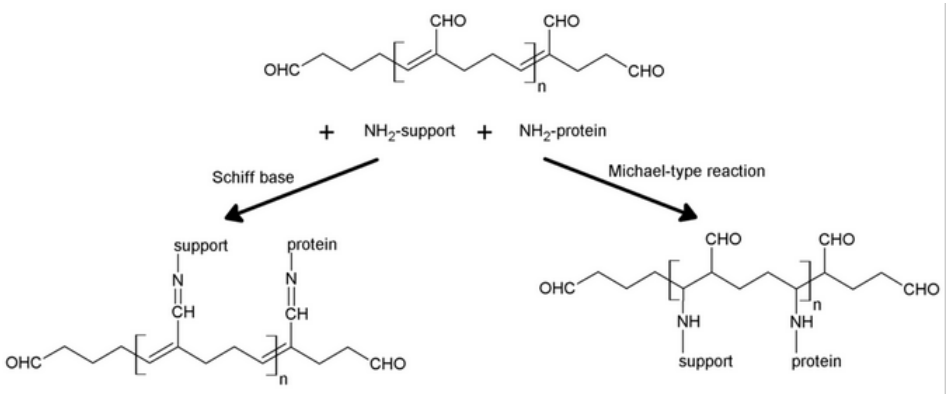

Figure 13 Crosslinking through functional groups

- Enzymatic crosslinking: this type of reaction is higly mild towards cells because of the absence of free radicals during the crosslinking; also, enzymes show a high degree of specificity thus avoiding side reactions during crosslinking.
  An enzyme which has been recently explored is horseradish peroxidase (HRP, figure 14), which catalyzes the coupling of phenols or aniline derivatives in the presence of hydrogen peroxide [18].

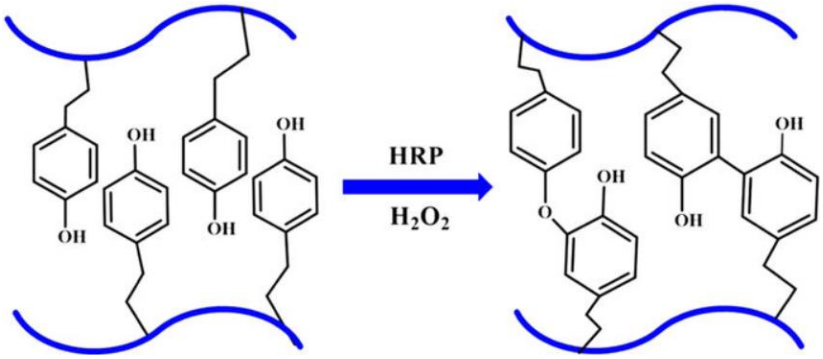

Figure 14 HRP reaction

- Physical crosslinking:
  - Stereocomplexation: Enantiomeric mixtures of polylactides (D- and L-PLA) co-crystalize into a stereocomplex [19-20] and were used in the design of injectable hydrogels- Hydrogel formation occurs by mixing two water-soluble polymers containing PLLA and PDLA blocks (figure 16).

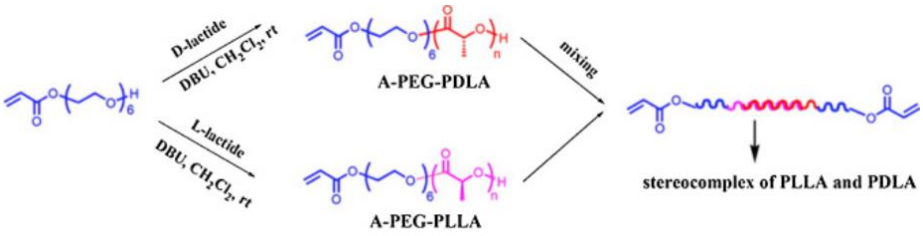

Figure 15 An example of stereocomplexation

  - Thermogelation: the process is triggered hydrophobic interactions upon a change of temperature [21].

  - Self assembly: the coiled-coil, one of the basic folding patterns of native proteins, has been used to design hydrogels. Gelation takes place when protein folding domains consisting of two or more helices wind together to form a superhelix [22].

  - Inclusion complexation: an example is between cyclodextrin (CD) and guest molecules, (figure 16)

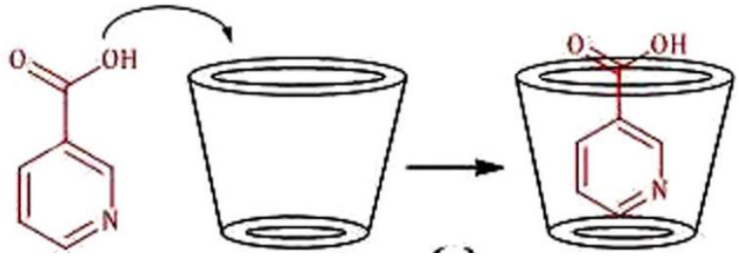

Figure 16 Ciclodextrine inclusion mechanism

1.5 Conclusions

Perfectly understanding tissue structure and composition is essential in order to design an optimal hydrogel, targeted to mimicking biological cues and specific chemistry of cartilage.
Usually, injectable hydrogels are prepared either from synthetic or natural materials that have their own pros and cons: synthetic polymers have the advantage to allow easily tunable properties and allow easy compositional variations; nevertheless they lack the necessary biofunctionality. Natural polymers, on the other hand, have high biocompatibility but show very high batch-to-batch differences.
These limitation have been a motivation to develop hybrid injectable hydrogels with precise physical, chemical and biological properties by combining synthetic and natural polymers.

1.6 Bibliography

[1] Alice J. Sophia Fox, MSc, Asheesh Bedi, MD,and Scott A. Rodeo, MD. The Basic Science of Articular Cartilage: Structure, Composition, and Function.

[2] M.B. Goldring, K. Tsuchimochi, K. Ijiri, J. Cell. Biochem. 97 (2006) 33– 44.

[3] E.B. Hunziker, T.M. Quinn, H. Hauselmann, Osteoarthritis Cartilage 10 (2002) 564–572.

[4]F. Barrere, T.A. Mahmood, K. de Groot, C.A. van Blitterswijk Advanced biomaterials for skeletal tissue regeneration: Instructive and smart functions.

[5]https://books.google.nl/books?id=toBDtreNf9cC&pg=PA136&lpg=PA136&dq=fibrocartilage%20histology&source=bl&ots=z7GnCFz37R&sig=b8bg23BJm5Idr9IW8b8LyIoajIM&hl=it&sa=X&ved=0ahUKEwjhrtnEovDYAhWJEVAKHUmhAc84ChDoAQhtMAk#v=onepage&q&f=false

[6] Saloni Tanna, Pharm.D. MPH. Priority Medicines for Europe and the World "A Public Health Approach to Innovation"

[7] Haq I, Murphy E, Dacre J. Osteoarthritis. *Postgrad Med J* 2003;79:377–383. Teitel AD, Zieve D.

[8] MedlinePlud Medical Encycolpedia. National Institutes of Health. “Osteoarthritis.” Last updated: Sept 26, 2011.

[9] Bitton R. “The Economic Burden of Osteoarthritis.” *American Journal of Managed Care* No 8. Vol 15: S230-S235. Sept 2009

[10] Langer R, Vacanti JP. Tissue Engineering. Science 1993;260: 920-926

[11] Raeber GP, Lutolf MP, Hubbell JA. Molecularly Engineered Peg Hydrogels: A Novel Model System for Proteolytically Mediated Cell Migration. Biophys. J. 2005;89: 1374-1388.

[12] Bryant SJ, Anseth KS. Hydrogel Properties Influence ECM Production by Chondrocytes Photoencapsulated in Poly(ethylene Glycol) Hydrogels. J. Biomed. Mater. Res. 2002;59: 63-72.

[13] Bryant SJ, Anseth KS. Controlling the Spatial Distribution of ECM Components in Degradable Peg Hydrogels for Tissue Engineering Cartilage. J. Biomed. Mater. Res. A 2003;64A: 70-79.

[14] Martens PJ, Bryant SJ, Anseth KS. Tailoring the Degradation of Hydrogels Formed from Multivinyl Poly(ethylene glycol) and Poly(vinyl alcohol) Macromers for Cartilage Tissue Engineering. Biomacromolecules 2003;4: 283-292.

[15] Bryant SJ, Durand KL, Anseth KS. Manipulations in Hydrogel Chemistry Control Photoencapsulated Chondrocyte Behavior and Their Extracellular Matrix Production. J. Biomed. Mater. Res. A 2003;67A: 1430-1436.

[16] Bryant SJ, Bender RJ, Durand KL, Anseth KS. Encapsulating Chondrocytes in Degrading Peg Hydrogels with High Modulus: Engineering Gel Structural Changes to Facilitate Cartilaginous

Tissue Production. Biotechnol. Bioeng. 2004;86: 747-755.

[17] Lutolf MP, Lauer-Fields JL, Schmoekel HG, Metters AT, Weber FE, Fields GB, and Hubbell JA. Synthetic Matrix Metalloproteinase-Sensitive Hydrogels for the Conduction of Tissue Regeneration: Engineering Cell-Invasion Characteristics. Proc. Natl. Acad. Sci. USA 2003;100: 5413-5418.

[18] Kobayashi S, Uyama H, Kimura S. Enzymatic Polymerization. Chem. Rev. 2001;101: 3793-3818.

[19] Loomis GL, Murdoch JR, Gardner KH. Polylactide Stereocomplexes. Polym. Prepr. (Am. Chem. Soc. Div. Polym. Chem.) 1990;31: 55.

[20] Tsuji H, Hyon SH, Y. Ikada. Stereocomplex Formation between Enantiomeric Poly (lactic acid)s. Macromolecules 1991;24: 2719-2724.

[21] Hennink WE, van Nostrum CF. Novel Crosslinking Methods to Design Hydrogels. Adv. Drug Deliver. Rev. 2002;54: 13-36.

[22] Yu YB. Coiled-Coils: Stability, Specificity, and Drug Delivery Potential. Adv. Drug Deliver. Rev. 2002;54: 1113-1129.

Chapter 2

2.1 Abstract

Native tissues are made up by modular building blocks which are cells surrounded by a thin layer of pericellular matrix (microenvironment), in turn surrounded by extracellular matrix (macroenvironment).
In this section, it is described how the presence of a soft material (which simulates cell laden micro droplet, the microenvironment) inside a much stiffer bulk material (which simulates the macroenvironment) influences the mechanical stability of the bulk.
In particular alginate droplets were used to simulate cell laden microgels, and agarose as a bulk.
In a stiffer agarose bulk, the concentration of alginate softer microspheres was tuned from 0 to 30% v/v in order to evaluate the effects of the soft gel over the mechanical stability (i.e. the E modulus) of the bulk.
Also, the micro droplets design was tuned to assess the influence of their elasticity and the size.
The results indicate that, for any elasticity and size of microgel droplets, when the amount increase, the influence of the bulk increases as well.
Furthermore, the effects are more remarkable when microgels are softer and their size is higher.
Finally, the microgel material was tuned as well, in order to evaluate if the influence over the bulk either depends on the microgel material itself, or only on the stiffness of the microgel.

2.2 Introduction

One of the main concerns in cartilage tissue engineering is the choice of an opportune biomaterial: once the scaffold is implanted, it will be subjected to the forces usually acting in that site. Physiologically such a tissue is subjected to very important loads that can be up to several times the body weight in the joints of lower limbs [1] such as hips and knees during walking, running and other daily living activities.

Then it is reasonable to state that a stiff material is necessary to bear such a high stress: a soft implant could break down and nullify the benefits of the surgery. Also, retrieving the fragments of the damaged scaffold inside a joint is not trivial.

This issue addresses the attention to a key point of cartilage tissue engineering itself: the dualism between stiff and soft material. In fact, as already mentioned, something stiffer is needed by the host organism in order to provide mechanical stability. On the other hand, something much softer is needed by cartilage cells, chondrocytes, in order to optimize their viability and enhance chondrogenesis [2].

As often is done in tissue engineering, the best way to design a functional construct is trying to copy what nature has already made.

Specifically, human native tissues are characterized by a multiscale modular design [3] [4]. The cells and matrices within are spatially organized into repetitive 3D building blocks endowed with biochemical and biophysical cues having functional impact down to the single cell level (figure 1)

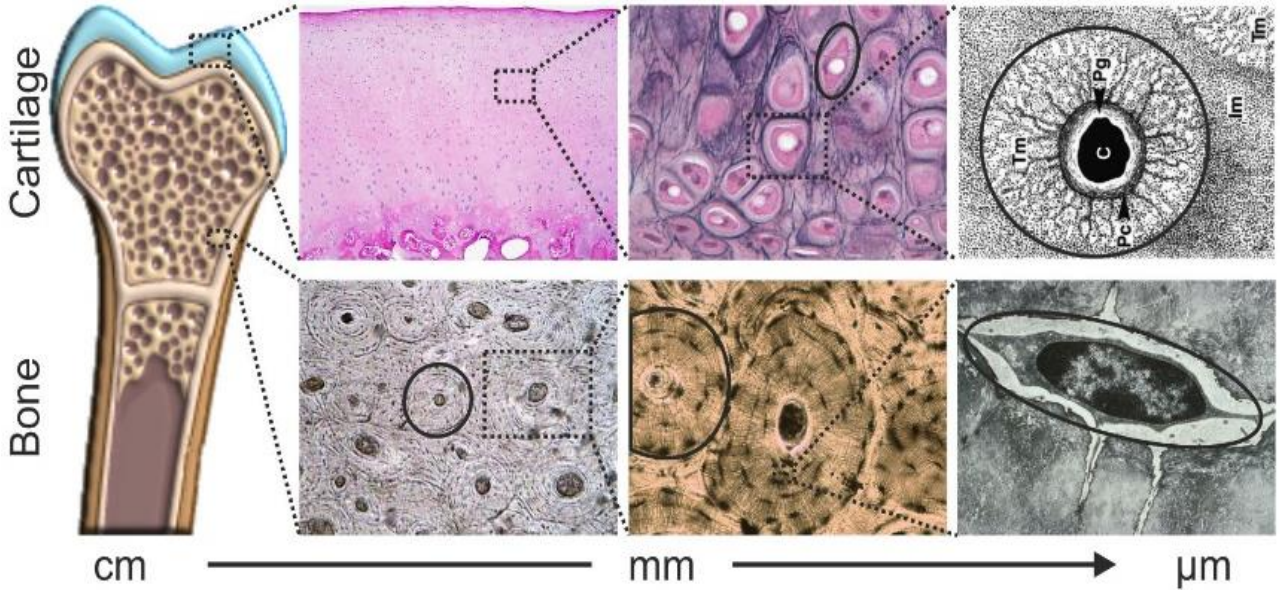

Figure 1 Tissue modular building blocks

[5].

In fact, these modules enable uncoupling of cellular and tissue micro- and macroenvironments, which is key to obtain the multifunctionality that is essential for proper tissue performance. Uncoupling the micro- and macroenvironments by integrating modularity is also expected to improve construct functionality of engineered tissues.[6]

Each chondrocyte is surrounded by a narrow pericellular matrix (PCM) that together with the enclosed cell(s) is referred to as a chondron.

Although the complete function of the PCM in cartilage has yet to be elucidated, growing evidence suggests that the PCM serves as a transducer of both biomechanical and biochemical signals for the chondrocyte.

The quantification of PCM biomechanical properties is technically challenging due to the low cell density of articular cartilage (Stockwell, 1971) and the micrometer length scale of the PCM (Hunziker et al., 1997; Youn et al., 2006) [7]. Nevertheless the biomechanical properties of this structure have only recently been measured. Techniques such as micropipette aspiration, *in situ* imaging, computational modeling, and atomic force microscopy have determined that the PCM exhibits distinct mechanical properties as compared to the ECM (Figure2).
As shown in the figure above, a tissue elasticity in the order of magnitude of hundreds of kPa is required to guarantee the stability of the joint (ECM), whereas a elasticity in the order of

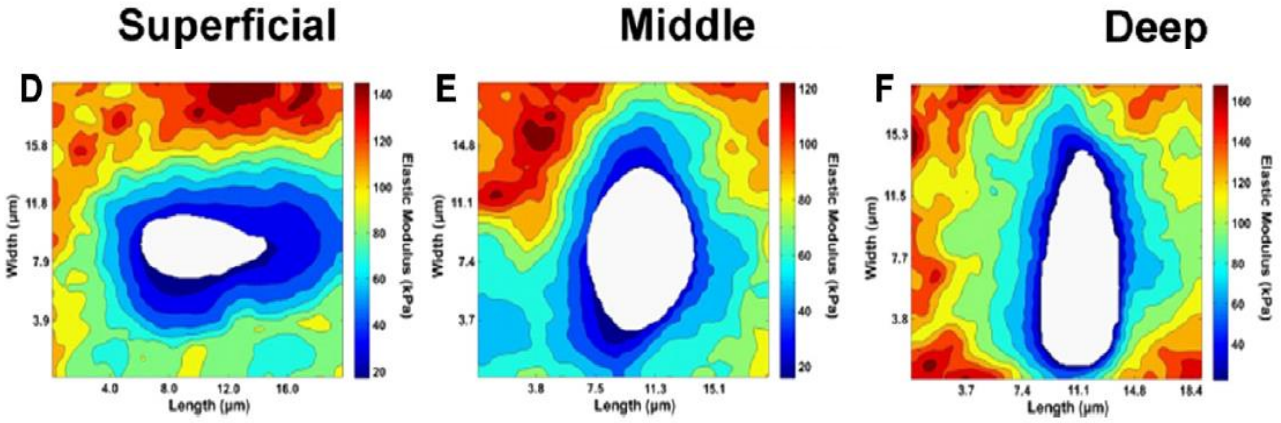

Figure 2 Chondrocyte micro niche and surrounding ECM

magnitude of few tens of kPa (10-25 kPa) is required to optimize chondrogenesis (Figure3)[8].

The final aim of the project is to engineer multifunctional tissues via a modular approach using

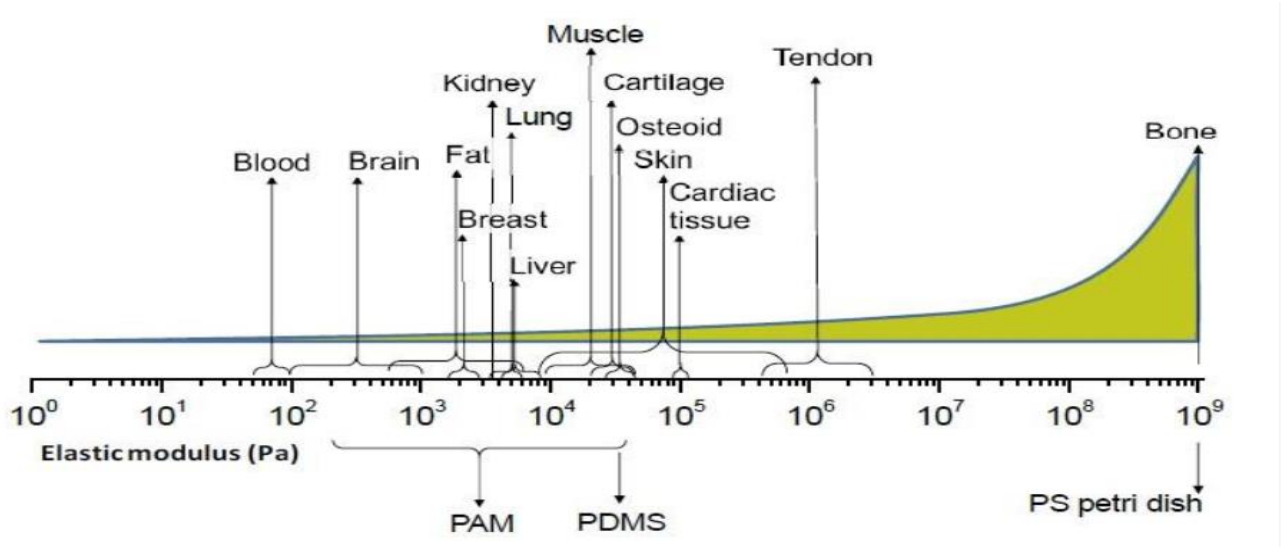

Figure 3 Optimum stiffness for human body tissues generation

bioink that comprises single-cell laden soft microgels in a stiffer macrogel representing the matrix. In this way micro- and macroenvironment are individually tunable according to the application. As cells covered by a thin layer of matrix are life's smallest functional units that can exist on their own, it is intuitive to create modular building blocks with single cell resolution. This biomimetic design is expected to provide biomaterials with the multifunctionality that is typically found in native tissues.

Now, to engineer a tissue, it is reasonable that the amount of soft microgel-coated cells inside the matrix is a crucial parameter in order to guarantee the mechanical stability of the bulk.
Purely by way of example, in a 1 cm^3 volume of stiff macrogel, the influence of a single coated cell (a sphere with a diameter of approximately 30µm) will be absolutely neglectable -owing to the negligible percentage of bulk volume which is occupied by the coated cell- and the Elasticity modulus of the bulk won't be affected. The same when the microgel spheres will be ten, or even one thousand. But what will happen when the coated cells will be several millions per ml of bulk, as occurs in native tissues? Is the bulk macrogel still capable to bear physiological loads? I.e. is the macrogel still strong enough? And if not, which is the maximum amount of coated cells that can be stored into a bulk without compromising its mechanical properties?
What is the influence of something much softer inside something much harder (Figure 4)?

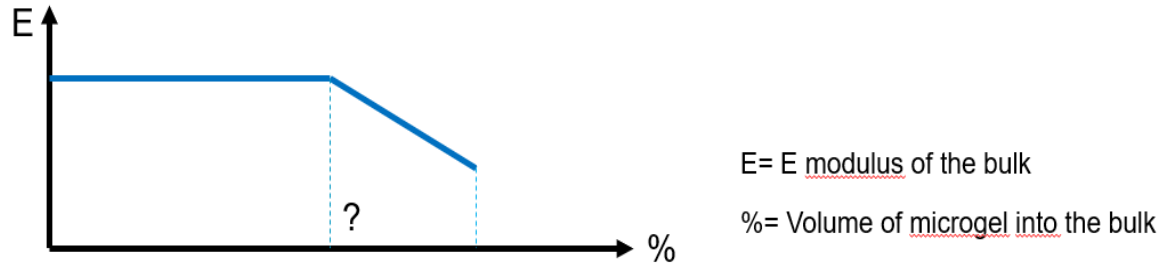

Figure 4 Expected trend of bulk stiffness

In order not to waste millions of cells, instead of using cells-laden microgel droplets, full microspheres of a soft biomaterial were used. In particular alginate was chosen, since with such material is possible to obtain a high amount of micrometric spherical droplets in a very reasonable time, as will be described.
To simulate the bulk material, we chose agarose, as it presents a remarkable stiffness at high concentrations an it gelates quickly at room temperature.
Specifically, the project is focused on the role of the stiffness of biomaterials involved. Then, in order not to introduce further variables, the micro- and macrogel will not be functionalized with chemical cues such as grow factors or other proteins.

2.3 Materials

Agarose powder was purchased by Thermofisher Scientific (UltraPure Agarose 1000, Invitrogen). Agarose is a polysaccharide, generally extracted from certain red seaweed. It is a linear polymer made up of the repeating unit of agarobiose, which is a disaccharide made up of D-galactose and 3,6-anhydro-L-galactopyranose. Agarose is one of the two principal components of agar, and is purified from agar by removing agar's other component, agaropectin (figure 5).

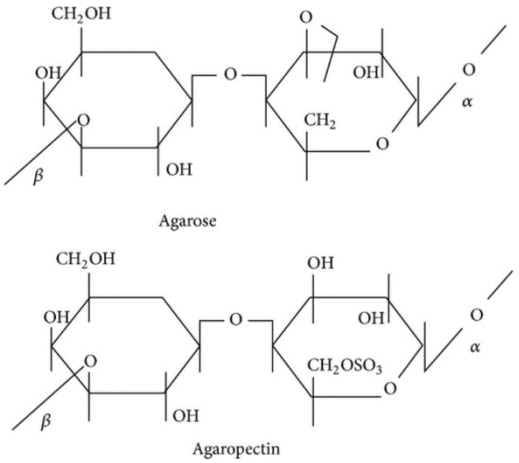

Figure 5 Agarose and agaropectin structure

Alginate was purchased by Wako (Sodium Algnate 80-120 cP). Calcium chloride was purchased by Sigma Aldrich. Alginic acid, also called algin or alginate, is an anionic polysaccharide distributed widely in the cell walls of brown algae, where through binding with water it forms a viscous gum. Alginic acid is a linear copolymer with homopolymeric blocks of (1-4)-linked β-D-mannuronate (M) and its C-5 epimer α-L-guluronate (G) residues (figure 6), respectively, covalently linked together in different sequences or blocks. The monomers can appear in homopolymeric blocks of consecutive G-residues (G-blocks), consecutive M-residues (M-blocks) or alternating M and G-residues (MG-blocks).

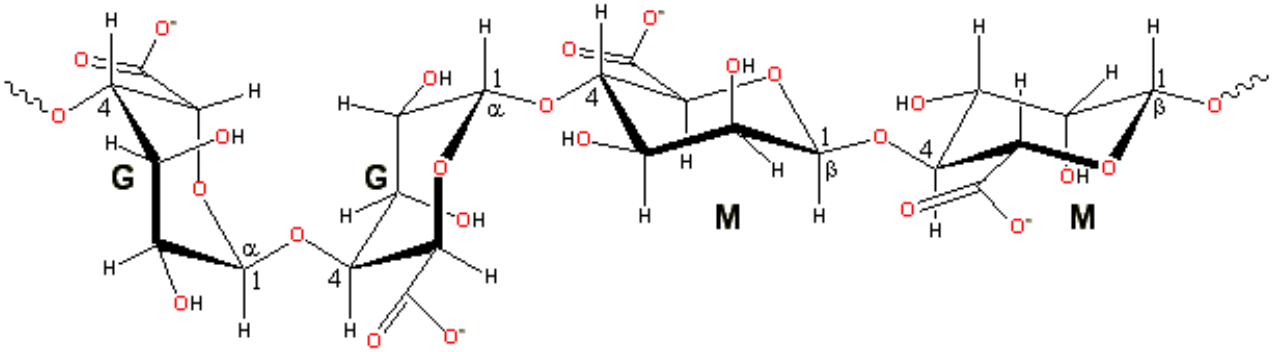

Figure 6 Alginate structure

Horseradish peroxidase (HRP) was purchased by Sigma Aldrich.
Hydrogen peroxidase was purchased by Sigma Aldrich.

2.4 Methods

2.4.1 PDMS MOLDS

A Poly Dimethylsiloxane (PDMS) solution was poured on the bottom of 14cm and 9cm Petri dishes and let at room temperature to allow the PDMS layer to spread homogeneously over the whole surface. The thickness of the layer was approximately 5mm. Afterwards the dishes were placed into an oven at 70°C for 3h. Also, a layer of PDMS with a circular hole in the center 3,5cm large was obtained; the temperature and time were the same described above (figure 7).
The reason why these molds were produced is that their hydrophobicity made much easier to detach the hydrogel samples compared to the plastic Petri dishes.

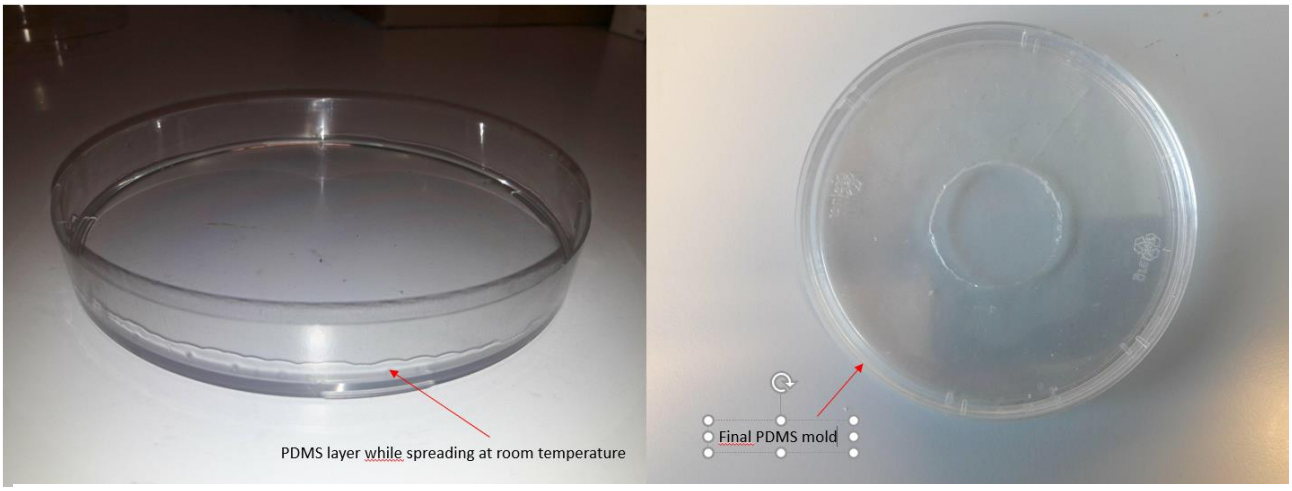

Figure 7 PDMS molds before (left) and after (right) curing.

2.4.2.1 Agarose

Agarose powder was dissolved at several concentrations w/v in DemiWater (DW) and weighted. Afterwards it was warmed up in a microwave reactor up to boiling point in order to completely and homogeneously dissolve the powder in the solution. Once the powder was finely dispersed, the solution was pulled out of the reactor and weighted again in order to keep constant the concentration of agarose with respect to the water. The amount of evaporated water was immediately restored by pipetting.
The hot solution was then pipetted 1,2ml per sample into the PDMS molds and gently shacked in order to obtain a homogeneously flat layer. The thickness of the layer was ~1.25mm, given the poured volume and the width of the circular mold.
The gelation time was a few minutes. Anyway, measurements were always performed 30 after samples production in order to guarantee complete gelation.

2.4.2.2 Fluorescent agarose

Fluorescent agarose powder was obtained by functionalizing normal powder as previously reported [15].
Briefly, the whole procedure was performed at 0-4°C with magnetic stirring:

- 0,85g of agarose powder was vaccum dried overnight
- 1,7g Nitrophenyl chloroformate were put into the reaction flask
- 25ml of anhydrous acetonitrile were poured
- Agarose powder was added to reaction flask
- In another flask, 3,06g of dimetthylaminopyridine (DMAP) were dissolved in an excess of anhydrous acetonitrile; once DMAP was dissolved, the compound was added to the first reaction flask

- 100mg of 6-aminofluoresceine were then dissolved in 20ml PBS. The solution was added to the first reaction flask and the product was shaked over weekend.
- Afterwards, the product was washed multiple times with PBS and acetone. The result was fluorescent agarose powder.

2.4.3 Alginate

A stock of alginate solution 2% w/v was produced pouring 4g of alginic acid powder into 200ml of DW and magnetically stirred overnight. Afterwards the content was poured into a jar and stored in the fridge at 4°C. For any further use, an aliquot from the stock will be diluted to reach the desired concentration.
To obtain gelation, a solution of calcium chloride was used to crosslink the alginate.
Nevertheless, crosslinking provokes the shrinkage of the gel. Also, the part of alginate solution in direct contact with calcium chloride solution often became irregular during crosslinking (figure 8).

Figure 8 Alginate shrinking in the mold

For these reasons obtaining a flat and regular alginate sample was not trivial and a protocol was necessary.
Into a 14cm Petri dish with a PDMS layer on the bottom, a 9cm plastic disc -with a hole in its center- was placed supported by ~1.5mm thick PDMS spacers. The alginate solution was then poured into the 14cm Petri dish and let spread all around and under the 9cm plastic disc.
Afterwards the construct was covered with the lid of the 14cm Petri dish, which was previously pierced with a drill. From the holes present in the lid, a solution of 0.1M $CaCl_2$ was poured with a serological pipette. As reported in the figure, the calcium ions could spread sidewards leaving the top and bottom surfaces flat because of the plastic and PDMS layers respectively.
The diffusion time was calculated according to the diffusion constant of Calcium ions, thanks to the calculator: http://www.physiologyweb.com/calculators/diffusion_time_calculator.html.
Afterwards the lid and its holes were sealed with tape in order to avoid water evaporation. After the necessary amount of time, the lid was removed as well as the 9cm plastic disc.
The result was a 9cm round and flat alginate bulk, from which smaller samples were obtained by punching the initial bulk (figure9).

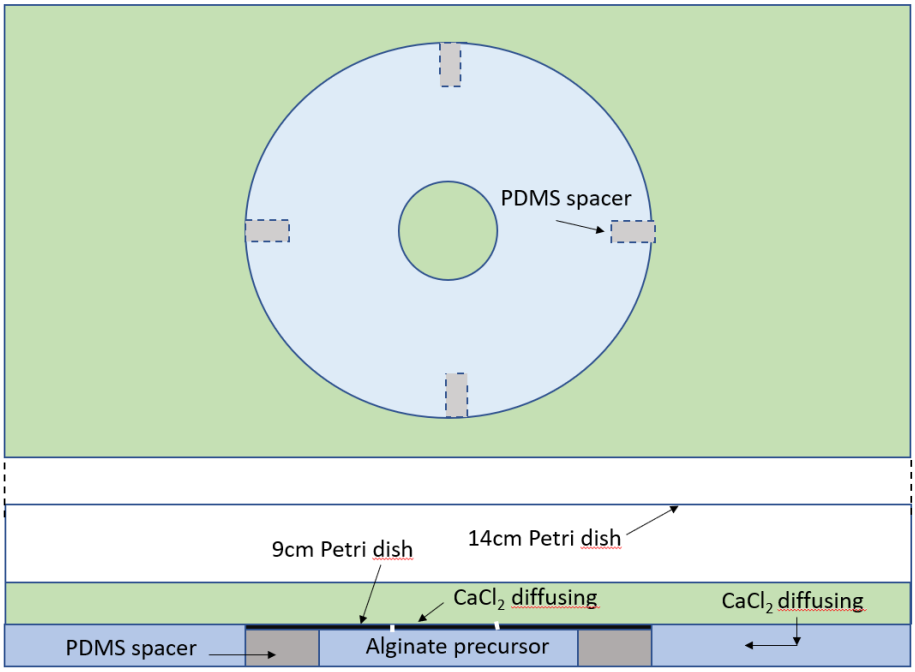

Figure 9 Representation of alginate gelation protocol

2.4.4 Rheology

All rheological experiments were carried out with a MCR 301 rheometer (Anton Paar, Figure 10) using parallel plates configuration (25 mm diameter, 0°) at 37°C in the oscillatory mode.
The strain and frequency used were 0.01% and 1Hz respectively.
In this way it was possible to directly extract the storage and loss moduli, G' and G'' respectively.
Afterwards, the Elasticity modulus was obtained through the formula:
$E=2G'(1+v)$
where E is the Elasticity modulus; G' is the storage modulus; v is the Poisson's ratio assumed equal to 0,5.
Also, to ensure the upper plate of the rheometer being perfectly in contact with the sample, a constant force F=0.5N was applied on the sample for the whole duration of the experiments as previously reported [10].
Before measurements, all the samples were cut in order to remove the excess of material and make them perfectly fit the round shape 25mm diameter of the rheometer upper plate.
Furthermore, during the experiments an oil trap (right picture) was applied to prevent water from evaporation and the consequent dehydration of samples.

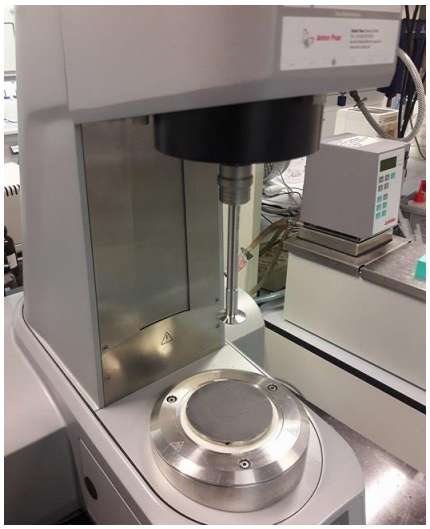

Figure 10A, MCR 301 rheometer (Anton Paar)

Figure 10B Oil trap: a few ml of water were poured around the sample to prevent dehydration, and a layer of oil was poured onto the water to prevent evaporation

The reasons why these particular strain (0,01%) and frequency (1Hz) were chosen are explained as follows.
Briefly, usually rheological properties of a viscoelastic material are independent from strain up to a critical threshold. Beyond this critical strain level, the material's behaviour is non-linear and the storage modulus declines [9] (Figure 11).

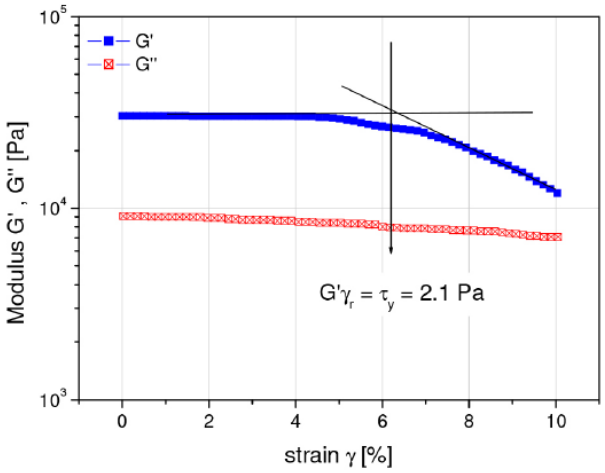

Figure 11 Generic trend of storage and loss modulus

So, measuring the strain amplitude dependence of the storage and loss moduli (G', G") is a good first step to take in characterizing visco-elastic behaviour: a strain sweep will establish the extent of the material's linearity.
Increasing the strain above the critical strain disrupts the network structure and the storage modulus will suddenly drop.
The material becomes progressively more fluid-like, the moduli decline, and G" exceeds G' eventually. The strength of the colloidal forces is reflected by tan δ = (G"/G'). A tan δ less than 1 suggests that the particles are highly associated due to the colloidal forces and sedimentation could occur: a high tan δ at given concentration suggests that the particles are largely unassociated.
After the fluid's linear viscoelastic region has been defined by a strain sweep, its structure can be further characterized using a frequency sweep at a strain below the critical strain γ_c.
Below the critical strain, the elastic modulus G' is often nearly independent of frequency, as would be expected from a structured or solid-like material. The more frequency dependent the elastic modulus is, the more fluid-like is the material (figure 12).

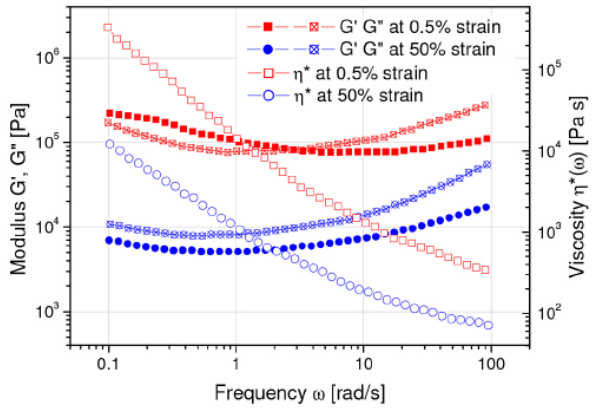

Figure 12 Generic trend of storage and loss moduli as functions of the frequency

2.4.5 IAMF

The alginate beads of any size (45-80-200-300 micron) and IPN alginate + DexTA beads were produced with the In Air Micro Fluidics (IAMF) platform as previously described [11].
Briefly, in IAMF, liquid microjets are manipulated and combined in the air after being actioned by a syringe pump and pushed through a tubing system culminating with two nozzles, as shown in figure 13 and 14.

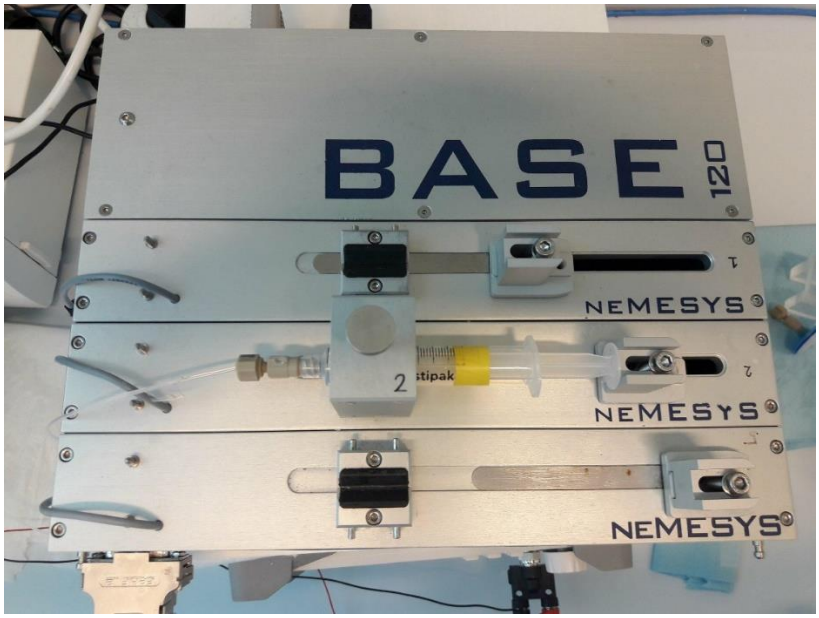

Figure 13 IAMF syringe pump; maximum deliverable linear force F= 290N.

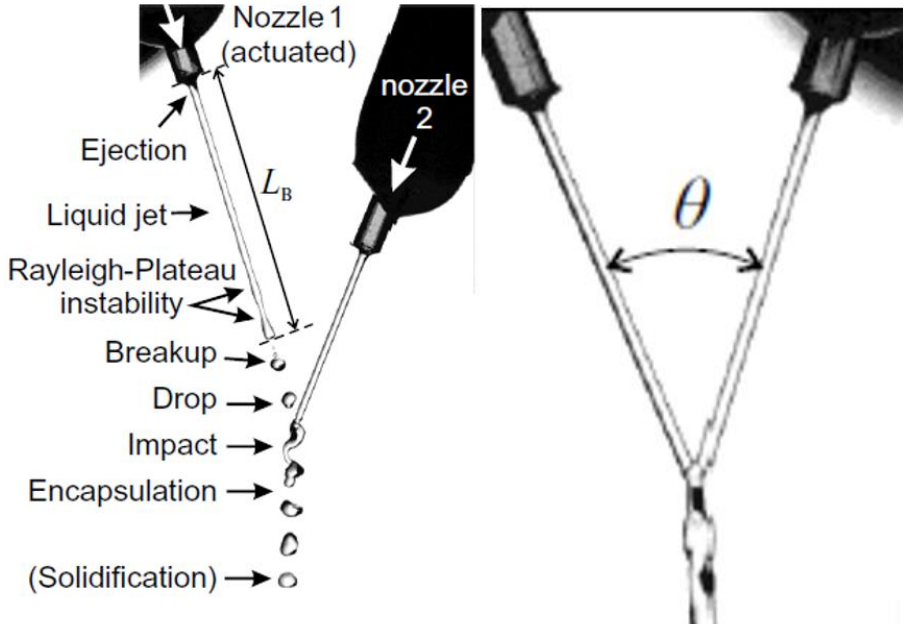

Figure 14 Phases of jet break-up

Droplets are generated by breakup of the liquid jet ejected from nozzle 1.
These droplets are monodisperse, as achieved by mounting the nozzle onto a vibrating piezoelectric element (sketched in figure 15) whose voltage, waveform and frequency could be opportunely tuned from a generator (figure 16). Specifically, for all the experiments an amplitude equal to $20V_{pp}$ in square wave, whereas the frequency was tuned according to the viscosity of the jet and the nozzle size.

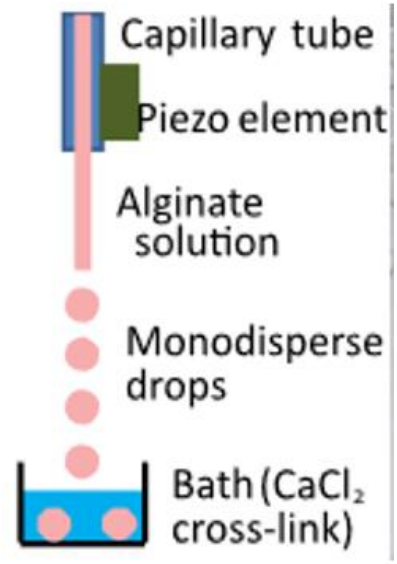

Figure 15 Setup scheme; Science Advances 2018

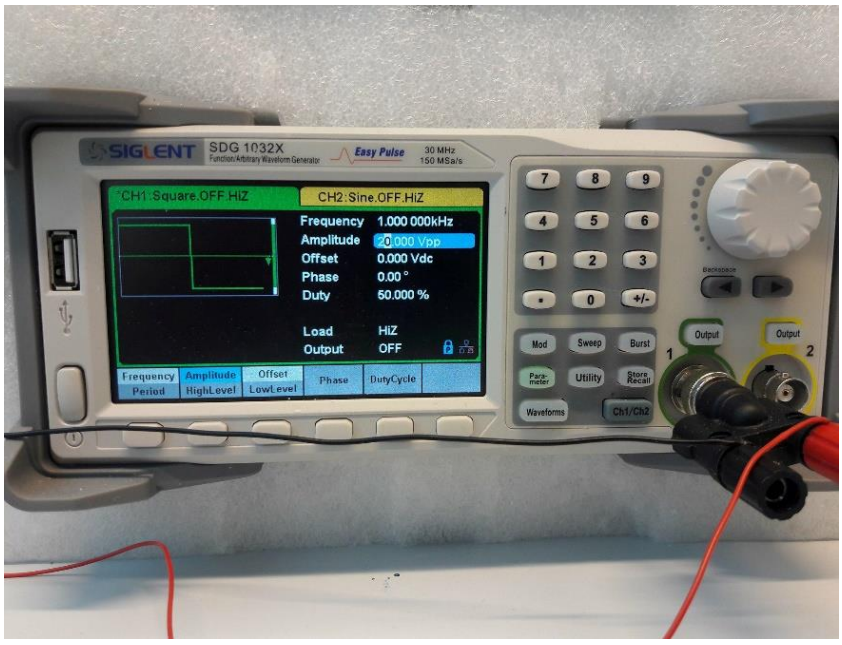

Figure 16 Frequency generator of piezoelectric element

The droplet train impacts onto an intact liquid jet that is ejected from nozzle 2 (figure 14), resulting in a compound monodisperse droplet train flowing downward. While flying in the air, the compounds react chemically or physically to form completely crosslinked droplets or particles (figure 17).

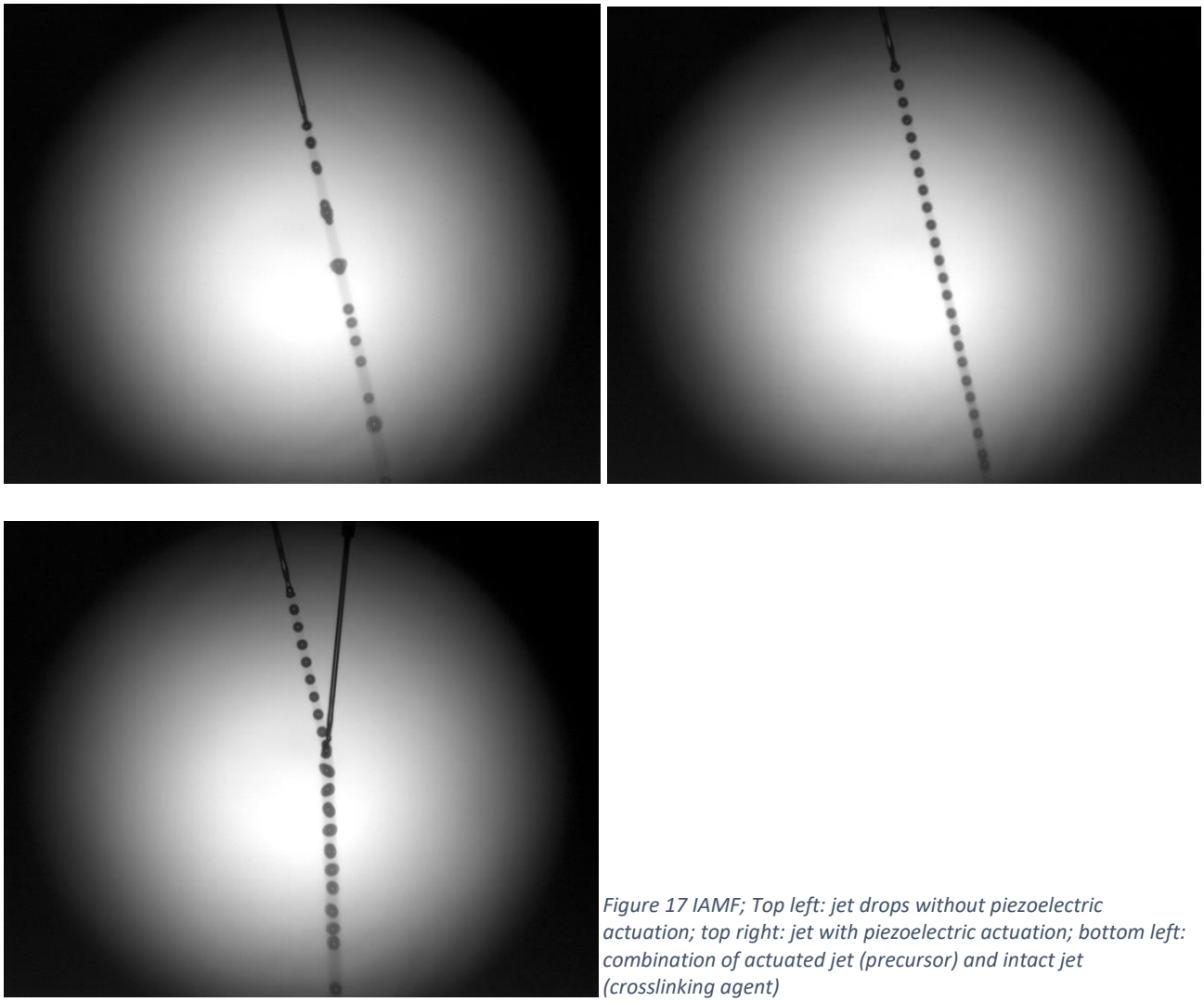

Figure 17 IAMF; Top left: jet drops without piezoelectric actuation; top right: jet with piezoelectric actuation; bottom left: combination of actuated jet (precursor) and intact jet (crosslinking agent)

In detail, what happens is sketched in figure 18: a droplet impacts onto a jet. Impact must result in coalescence, whereas droplet bouncing, stretching, or splashing must be prevented [11].

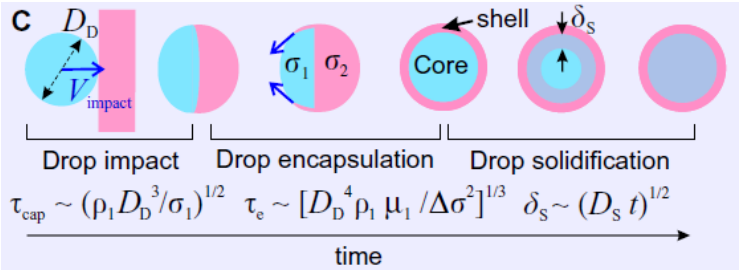

Figure 18 Sketch of particles generation; Science Advances 2018

Furthermore, maintaining the production of spherical particles is promoted if the droplet remains spherical during impact.
Both these conditions are met if capillary forces dominate inertia, that is, for impact Weber numbers $W_{impact} = (\rho_1 D_D V_{impact\,2})/\sigma 1 \lesssim 3$, where ρ_1 ,σ_1 , and D_D are the droplet density, surface tension, and diameter, respectively [12, 13].
The impact velocity $V_{impact} = V_1 \sin\theta$ depends on the impact angle θ and the ejection velocity V_1 of jet 1.
The crucial trick that prevents the droplets ejected from nozzle 1 from merging during flight is to ensure their encapsulation by the intact jet. To drive this in-air encapsulation, the surface tension of the encapsulating liquid (pink) was reduced with respect to the one of the hydrogel precursor (blue)by adding ethanol.
Both impact and encapsulation are completed in the air before collection or deposition, which happens typically ~100 ms after in-air impact.

The droplet or particle sizes could be tuned according to the needs by varying the nozzle diameter and actuation frequency (figure 19).

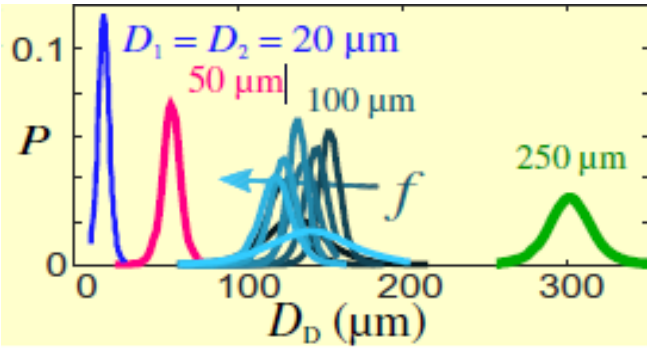

Figure 19 Effect of actuation frequency and nozzle diameter on particles diameter ; Science Advances 2018.

The result was the production of monodisperse beads of several diameters ranging from 80 to 300 micron (figure 20).

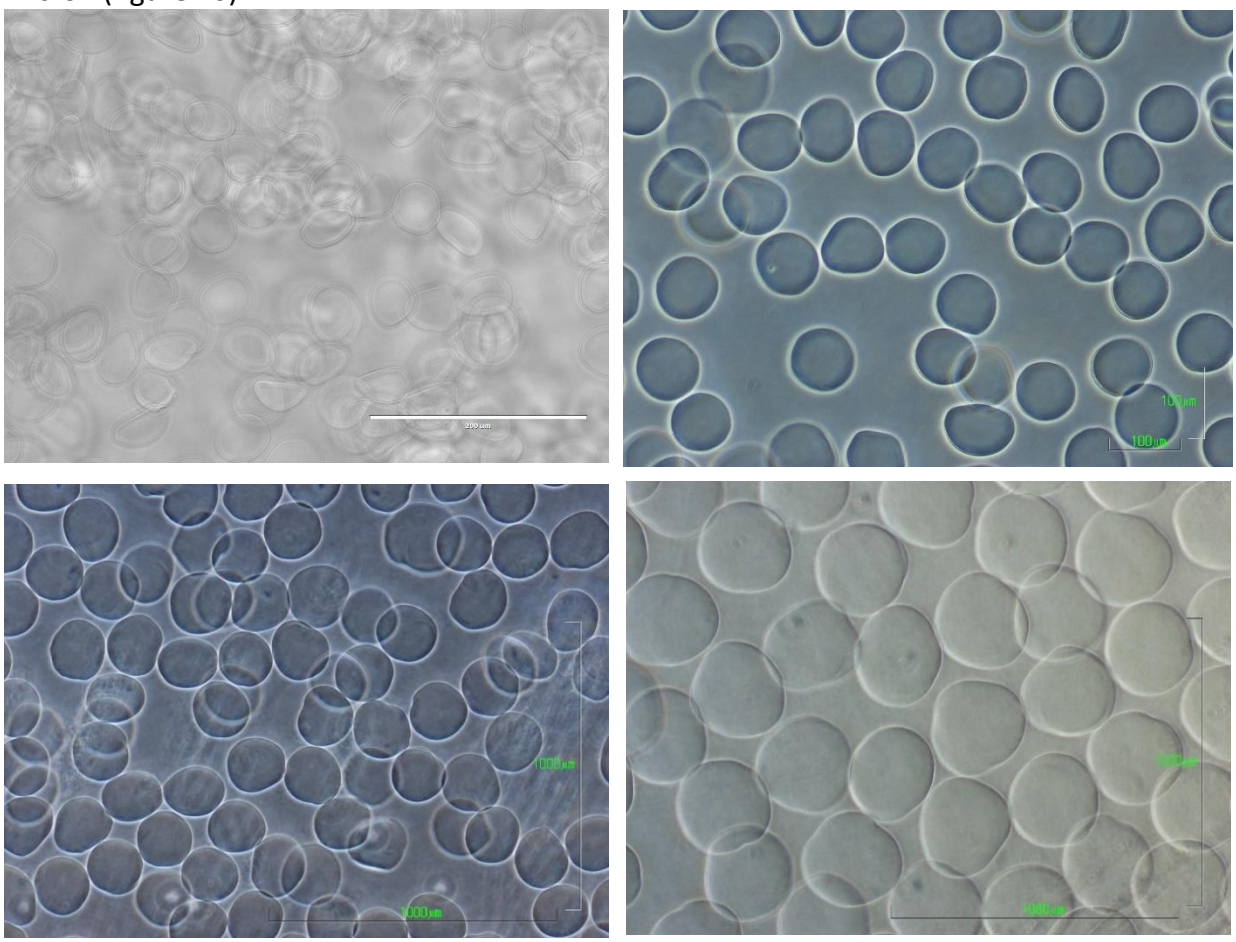

Figure 20 Optical microscope images of 45 (top left), 80 (top right), 200 (bottom left) and 300 (bottom right) micron alginate beads obtained with IAMF platform

Finally, a few images of the whole setup are reported.

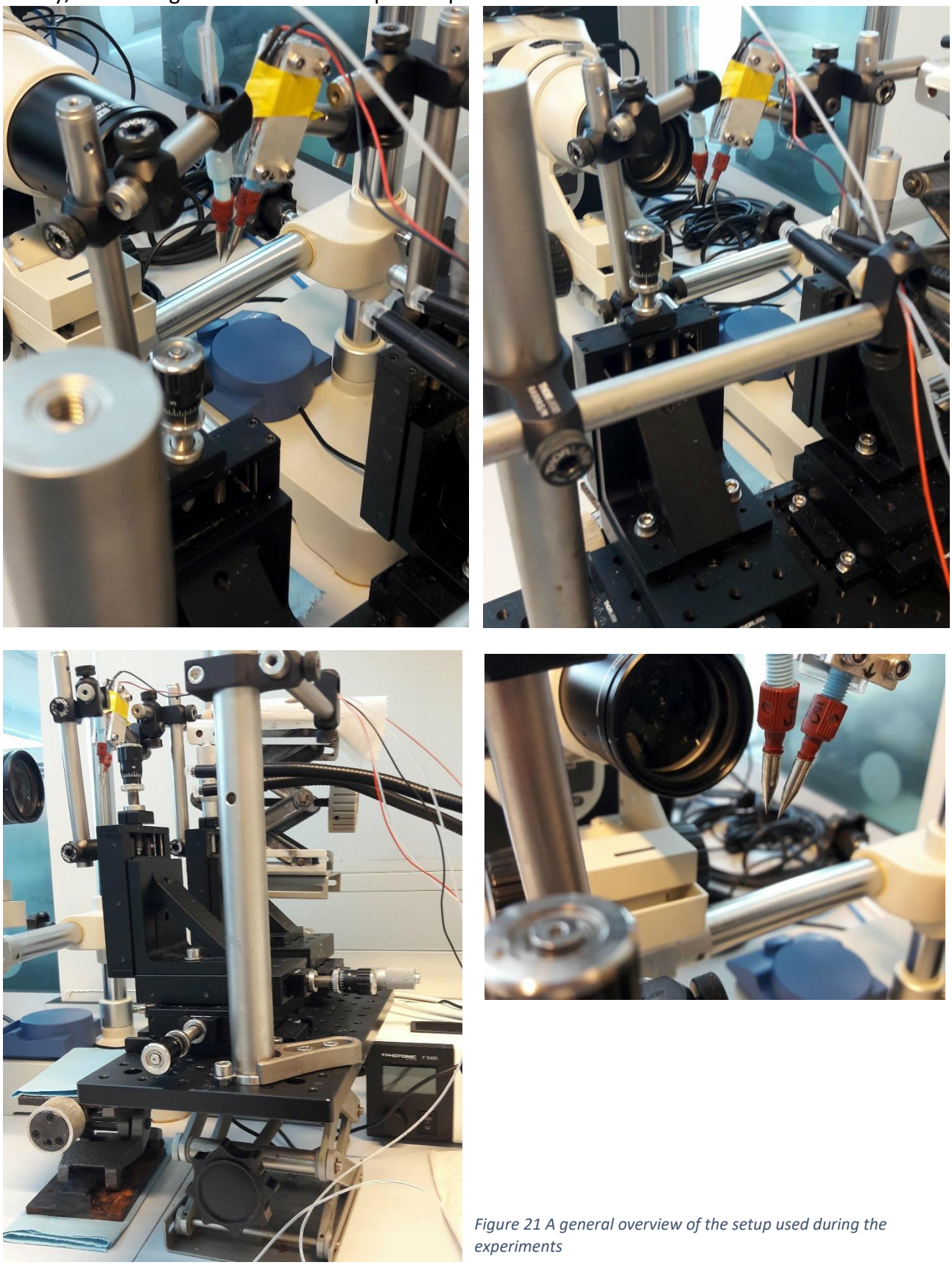

Figure 21 A general overview of the setup used during the experiments

2.4.6 Mixing agar and alginate

In order to assess the effects of softer beads inside a stiffer bulk, the two materials were mixed. To achieve such a goal, the bottom plate of the rheometer was warmed up to 100°C in order to prevent gelation of agarose.
Two stock solutions of agarose (5% and 7.5% w/v) were used.
Once the plate reached the proper temperature, the agarose gel was warmed up into a microwave reactor and weighted before and after. The evaporated amount of water was restored to keep the concentration of the agarose constant.
Afterwards, a metal mixing chamber with a volume of a few millilitres (Figure 22) was placed on the warm bottom plate of the rheometer, and once it was at the same temperature, the liquid hot solution of agarose was poured into the chamber. Then, the desired amount of beads was added for any testing condition.

Figure 22 Metal mixing chamber

The bulk hydrogel used for all the experiments consisted of 4% w/v agarose.
After production with IAMF, the alginate beads were collected into a tube and stored into a 0.1M $CaCl_2$ solution. Before the usage, the supernatant was removed by pipetting. Nevertheless it was not possible to remove the liquid present between the beads. With a random packing, a density equal to 50% was assumed. Then, when mixing, the beads were added by pipetting them out of the tube
For each condition, the experiments was performed in triplicate. Then three samples (1,2ml each) were produced. Since part of the material stuck to the chamber walls during the mixing procedure, the volume of material used during the production was higher than 1,2x3=3,6. Specifically, 4,5ml were used.

Right below, every condition is reported.

8% v/v beads

- 2x0,83ml agar stock solution 5%
- 0,72 ml beads solution (0,36ml beads + 0,36ml liquid)
- 0,47ml Demiwater
- 2x0,83ml agar stock solution 5%

The total volume of the beads was 0,36ml; the bulk volume was 4,5-0,36=4,14ml.
The amount of agar 5% was 3,32ml. Reasonably, 3,32x5%=C%x4,15 where C=4 is the concentration of the diluted solution.

16%vol

- 1x1ml agar stock solution 5%
- 2x0,75ml beads solution
- 2x1ml agar stock solution 5%

25% vol

- 0.9ml agar stock solution 7,5%
- 3x0,75ml beads solution
- 0,45ml Demiwater
- 0,9ml agar stock solution 7,5%

30%vol

- 0,84ml agar stock solution 7,5%
- 3x0,9ml beads solution
- 0,12ml Demiwater
- 0,84ml agar stock solution 7,5%

All the solutions, after having being poured into the mixing chamber were gently mixed with a metal spatula to make the moisture very homogeneous. Afterwards the content was pipetted out in three PDMS molds in the quantity described above.

2.4.7 IPN DexTa-Alginate

A precursor solution made up by two components was prepared and then crosslinked in the air with IAMF platform.
Briefly, the first component was the gel precursor, the final concentration is reported:

- 0.25%alginate
- 5% DexTa
- 25U/ml HRP
- H_2O

The second solution's composition was:

- 0.2M $CaCl_2$
- 0.05% w/w H_2O_2
- 10% Ethanol

The mechanical properties of the material were measured by producing a bulk with the same protocol used for the alginate and the solutions listed above were used.

2.5 Results and discussion

2.5.1 Agarose

The Elasticity modulus of agarose was proportional to the polymer concentration, and the results are shown right below.

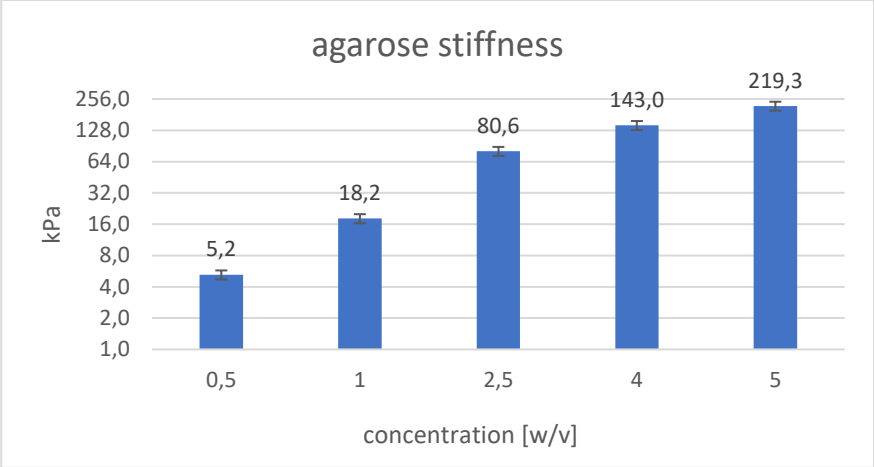

Figure 23 Agarose stiffness as a function of the concentration

The data are quite in line with the ones previously reported in literature [14] right below (Figure 24-25). Nevertheless a characterization was necessary, as the polymer properties can slightly change from one powder to another.

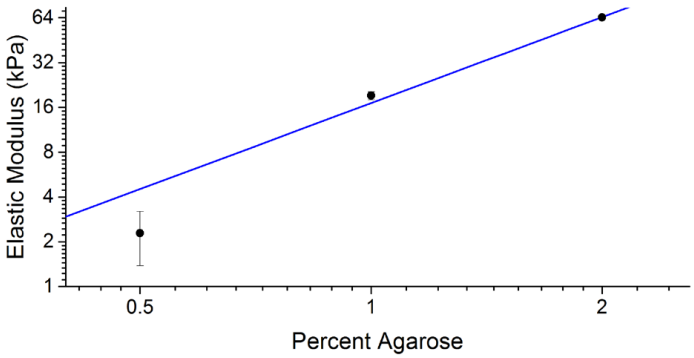

Figure 24 Agarose stiffness (Mechanical Characterization of Hydrogels, by Benjamin and Stadnick)

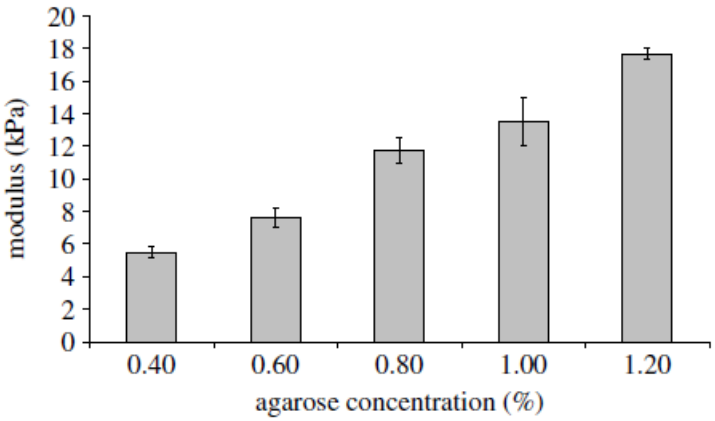

Figure 25 Agarose stiffness (Characterizing the viscoelastic properties of thin hydrogel-based constructs for tissue engineering applications, by Ahearne et al)

2.5.2 Alginate

The elasticity of alginate hydrogel, as well as for agarose, was directly proportional to the polymer concentration. The results are reported right below:

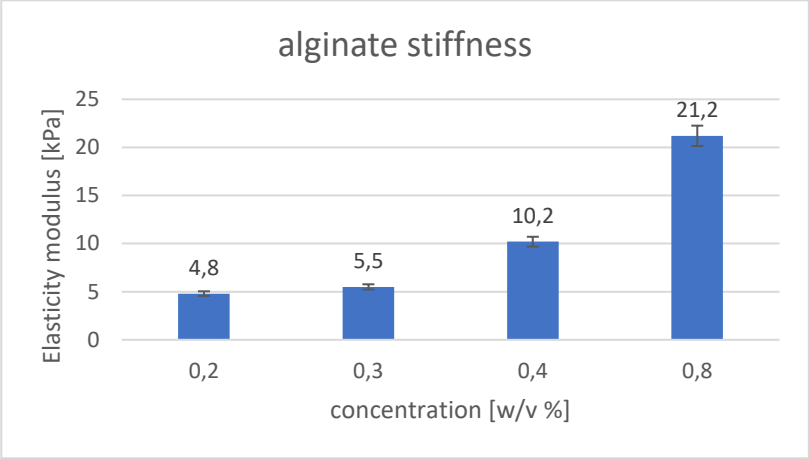

Figure 26 Mechanical properties of alginate

Also in this case, the findings were comparable with the results previously reported in literature (figure 27):

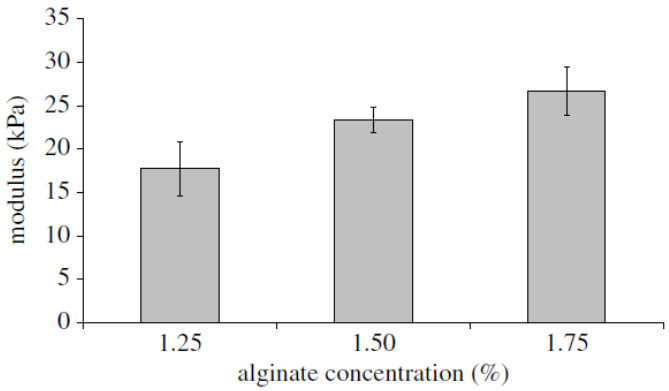

Figure 7. Young's modulus of the alginate at different concentrations (n=3).

Figure 27 Mechanical properties of alginate reported in literature [14]

In this case is possible to notice that the alginate used for the experiments was slightly stiffer, as a similar E modulus was obtained with lower concentration. The main reason of the difference is most likely the different ratio between Guluronic and Mannuronic residuals, as a higher presence of Guluronic blocks results into higher mechanical properties.

2.5.3 Agar bulk and alginate beads

2.5.3.1 Tuning beads' elasticity

The results are reporting the effects of soft beads/microdroplets with the same size inside the same stiffer bulk when the elasticity of the beads is tuned.
The data points which have been considered were 15% and 30% v/v. The reason why these percentages were chosen is that:

- 15%: at the beginning it was required to assess the influence of the beads at low percentages, i.e. 5-10-15%. Reasonably, the first percentage to be evaluated was 15%, since if no influence was noticed, it would have not been necessary check even lower percentages; it this way it was possible to save both time and material.
- 30%: it was the highest volume percentage reachable using 7.5% w/v agarose. In fact, because of the liquid present in the beads' solution, the agarose will be always diluted, and with percentages higher that 30% the final concentration of agarose bulk would have been lower than 4%. An option would have been using an agarose stock concentration higher that 7.5%, but it would have been necessary to increase a lot the concentration of the stock in order to increase just a few percentages points the amount of beads storable in the bulk.
  Furthermore, it was noticed that for more concentrated agarose solutions, physically pipetting such a viscous solution is everything but trivial.

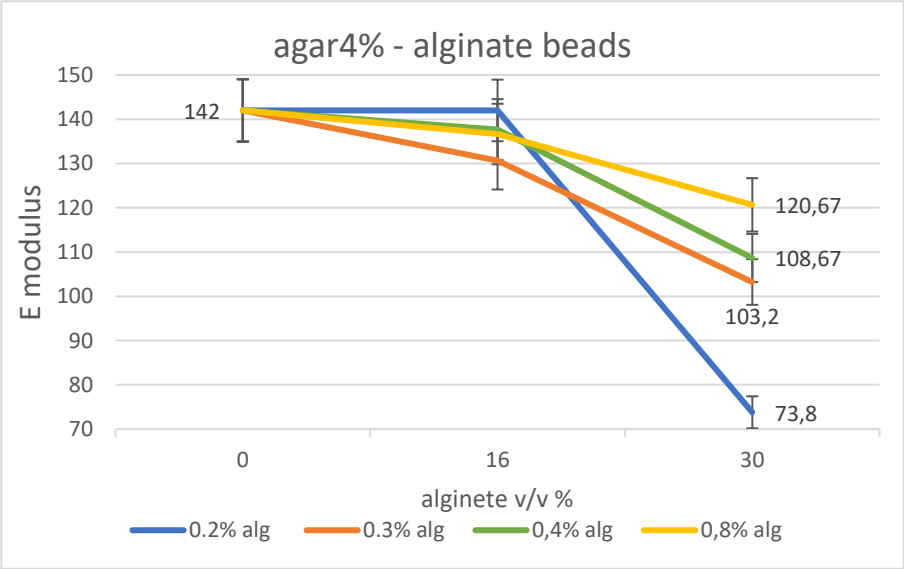

Figure 28 Elasticity modulus of the bulk as a function of the volume percentage of the beads when their stiffness is tuned

In figure 28 is possible to notice that until 16%, no remarkable mechanical influence is noticed for any elasticity of the beads.
The values of Elastic modulus are slightly lower than the stiffness at 0%, but the difference (<10% with respect to the initial value) is reasonably due to the variability between samples.
On the other hand, at higher percentages it is evident that the influence is even end even more important when the beads get softer.

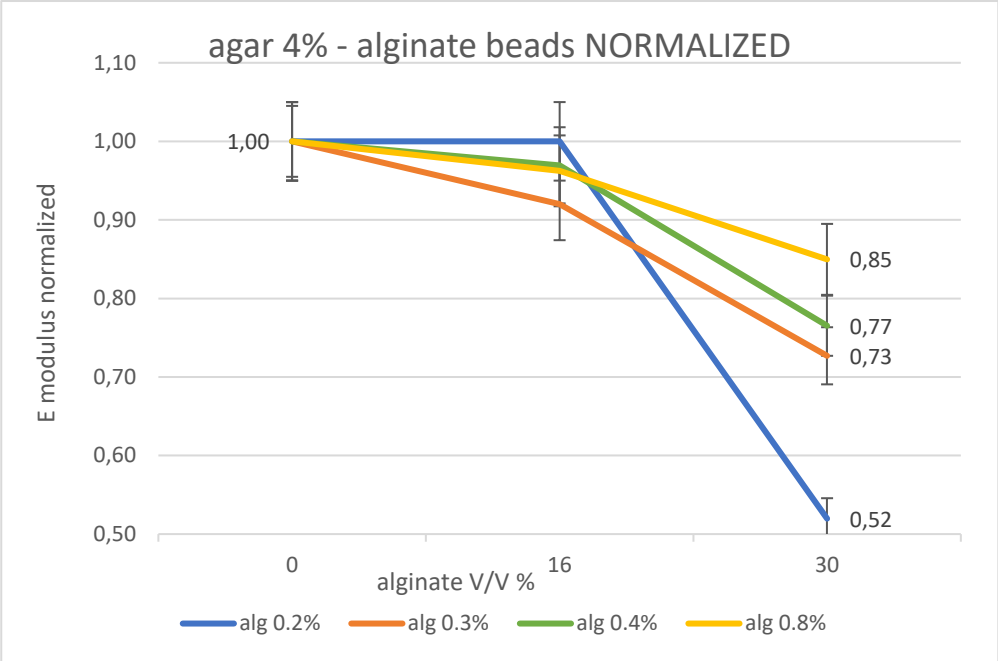

Figure 29 Normalized stiffness of the bulk as a function of the volume percentage of the beads when their stiffness is tuned

In particular, it deserves to be highlighted that when the alginate concentration is halved at higher values (from 0,8 to 0,4% and consequently E modulus of the beads decreases by 50% from ~20 to ~10 kPa) the difference of influence over the bulk is much less evident if compared with the effects of halving the alginate concentration at lower values (i.e. from 0,4 to 0,2% and consequently E modulus of the beads decreases by 50% from ~10 to ~5 kPa).
In fact, tuning from 0,8 to 0,4% entails a percentage decrease of 85-77=8% of E modulus with respect to the initial value.
But when alginate is tuned from 0,4% to 0,2% the consequence is a percentage decrease of 77-52=25% of bulk E modulus with respect to the initial value.

2.5.3.2 Size

Hereby, are reported the results of the influence over bulk mechanical properties when the elasticity of the beads is kept constant and the size is tuned.
The data points selected are 8-16-25-30% v/v. The two data points 16-30% were selected for the reasons previously described. Then two further data points 8-25% were arbitrarily chosen in order to have an approximately constant percentage gap between all data points.

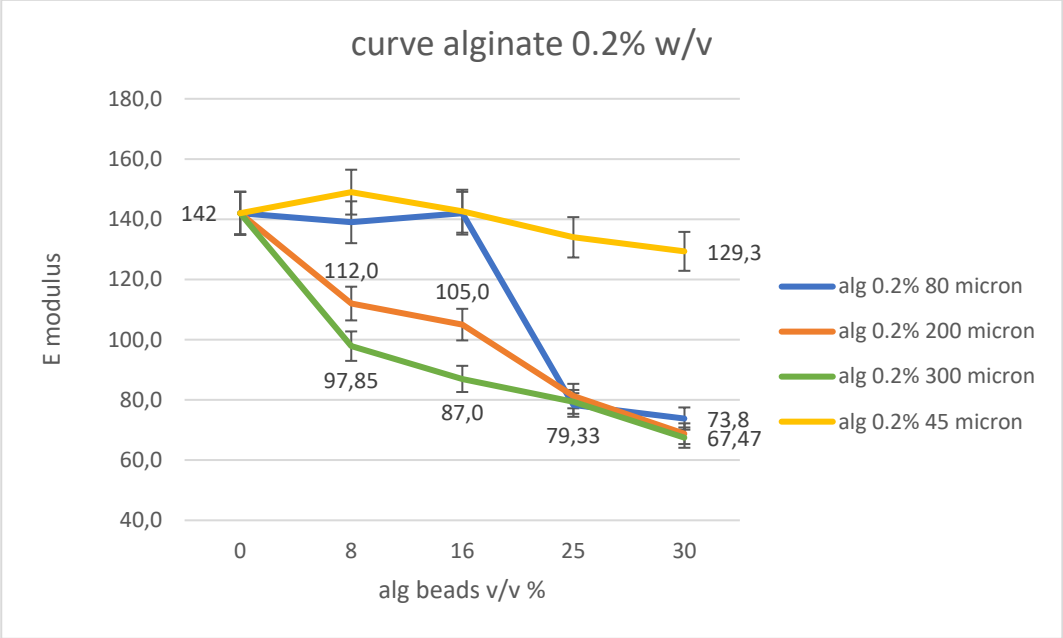

Figure 30 Elasticity of the bulk as a function of the volume of the beads and their size

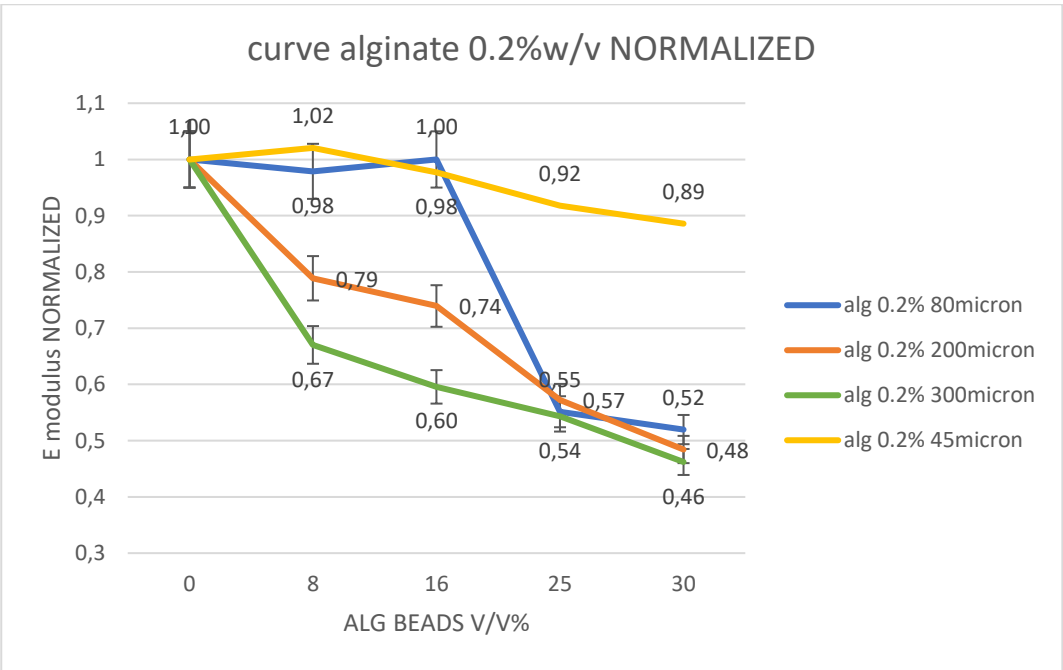

Figure 31 Normalized elasticity of the bulk as a function of the volume of the beads and their size

First of all, what can be noticed is that the situation is quite opposite with respect to the previous case: in the picture is possible to notice a remarkable difference of mechanical influence when beads of different sizes are present at low concentrations.
On the other hand, when the volume amount is higher the influence of the beads is approximately the same for every size apart from 45µm beads.
Supposedly, the reason of these result is that for low concentrations in the bulk are present relatively a few beads, representing discontinuity points. From the theory of mechanics, such points represent spots where the stresses are much higher than elsewhere.
When these points are small enough (i.e. 45 and 80µm), most likely, the bulk can bear the increase of stress. But when the dimensions of the beads increase, the bulk gets even and even more influenced by the amplification of stress in such spots.
As far as it concerns the influence at higher concentrations, the reason why the mechanical properties showed by the bulk are the same for every size (apart from 45 µm) is that when such a high percentage of the volume is occupied by something 10 fold softer than the bulk, this will be affected independently from the dimension of the points of discontinuity.
About the curve with 45µm beads, is reasonable to expect to notice the same influence over the bulk, but with higher v/v percentage: i.e. a trend similar to the curve with 80 µm beads, but with the critical threshold shifted to higher values (then to the right).

2.5.3.3 Different biomaterial

The goal of this experiment was to assess if it is possible to generalize the results previously reported or they are valid only for that particular biomaterials. In order to do that the material of the beads was changed (an IPN of alginate/Dex-Ta), whereas the bulk material didn't change.
The mechanical measurements performed over the IPN Dex-Ta/Alginate gave as a result a stiffness almost identical to the one of the 0,4% alginate hydrogel as reported in figure 32.

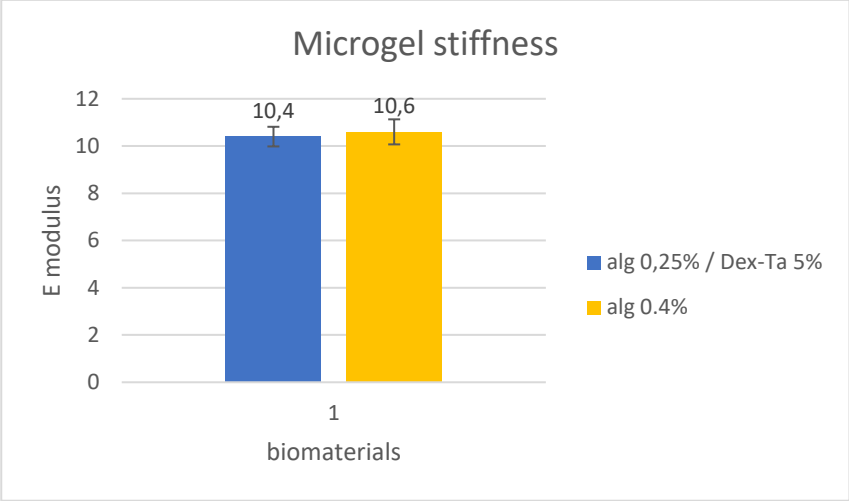

Figure 32 Stiffness of IPN alginate+dextran compared with 0,4% alginate

Reasonably, if the hypothesis were right, the mechanical influence over the bulk should be comparable.

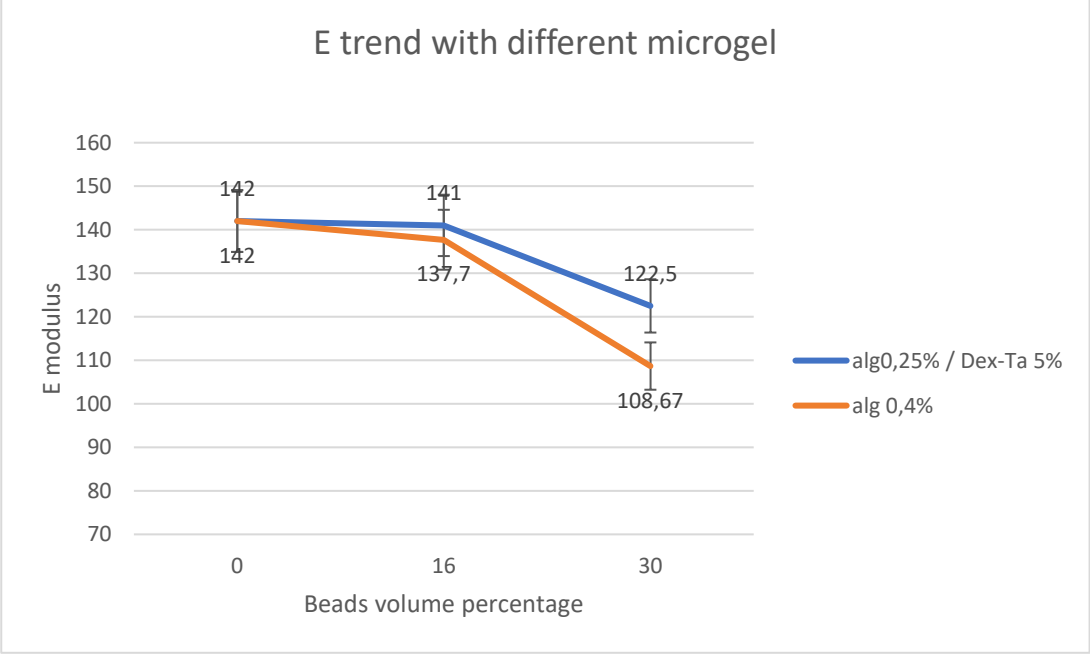

Figure 33 Comparison between curves of 0,4 alginate and IPN

In fact, the results confirmed that the influence is almost identical for lower concentrations (figure 33), but when the concentration increases the influence is not comparable anymore. The conclusion than can be drawn is that a different biomaterial can influence mechanical stability at high concentrations, but not when the concentration is lower than a critical threshold.

2.6 Results validation

To validate the previously presented results, a further point which needed to be investigated was the possible interpenetration of agarose polymer chains into alginate softer beads.
Three scenarios are possible:

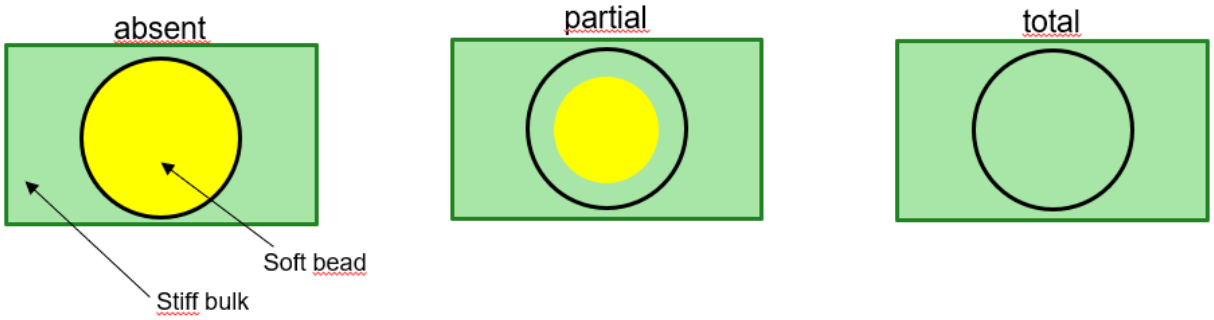

Figure 34 Possible scenarios in case of polymer interpenetration

The reason why this was done is dual:

- Firstly, in case the interpenetration is considerable, it wouldn't be true anymore that -for example- when the diameter of the beads is 80µm, their influence over bulk mechanical properties is negligible up to 16% V/V: if 50% beads' volume was penetrated by agarose, their actual volume percentage with respect to the bulk would not be 16%, but 8. In such scenario the results would be biased.
- Secondly, as will be described in the next chapter, in case of single cell laden microgels, the thickness of cell coating is ~5-10µm: if the radial penetration of the stiffer bulk material was deeper, it wouldn't be true anymore that cells are in contact with a softer substrate optimal for chondrogenesis, but they would be in contact with the stiffer bulk material, and this could induce apoptosis.

In order to investigate it, the method which was used consisted of making the bulk material fluorescent, whereas softer beads were not modified.
Right below, the picture shows the difference between normal and fluorescently modified agarose powder.

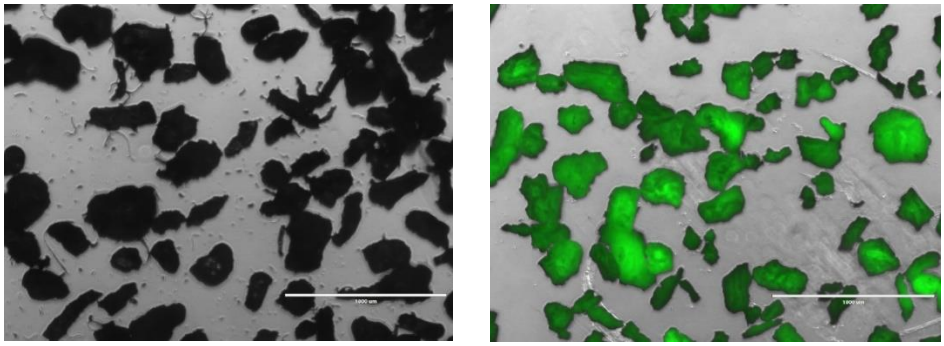

Figure 35 Comparison between normal agarose powder and 6-aminofluoresceine functionalized agarose powder

A new batch of alginate beads was produced with IAMF platform and the diameter of the microspheres was quantified with ImageJ software, resulting to be 66µm.

A picture of the beads is reported:

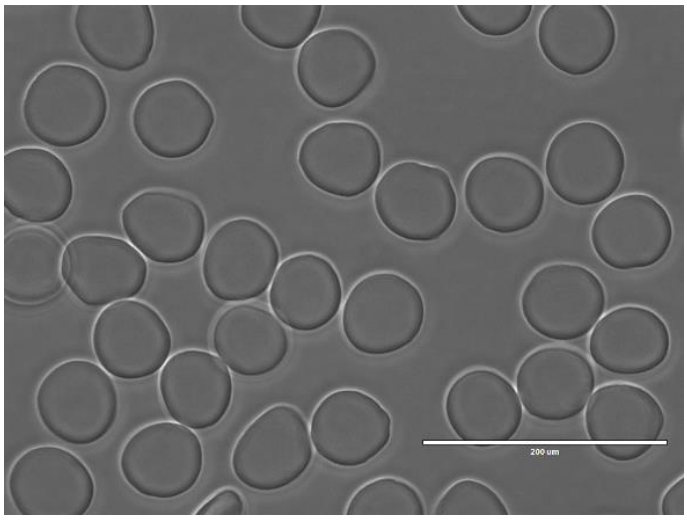

Figure 36 Monodisperse alginate non-fluorescent beads

To produce the samples used for the experiment, agarose powder was dissolved in demiwater and magnetically stirred at high temperature (90°C) in order to produce a homogeneous fluorescent hydrogel.
Then, alginate non-fluorescent beads were added to fluorescent agarose in order to produce a bulk 4%w/v with 16%v/v beads. The samples' thickness was approximately 100 µm.

Immediately after the production, the samples were imaged with confocal microscopy technique in order to scan the construct one plane at a time: in this way is possible to visualize the green fluorescent bulk and darker circles where non-fluorescent beads are present (see schematic picture right below).

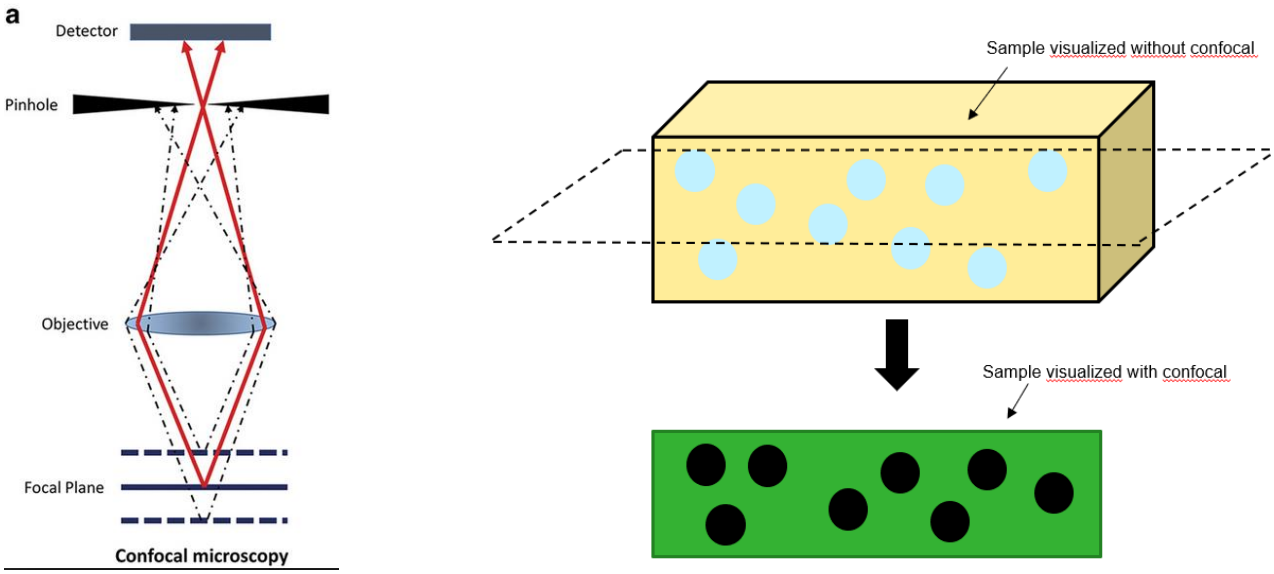

Figure 37 Schematic representation of confocal microscopy (left) and how the sample is imaged (right)

In this way it was possible to retrieve the necessary data.

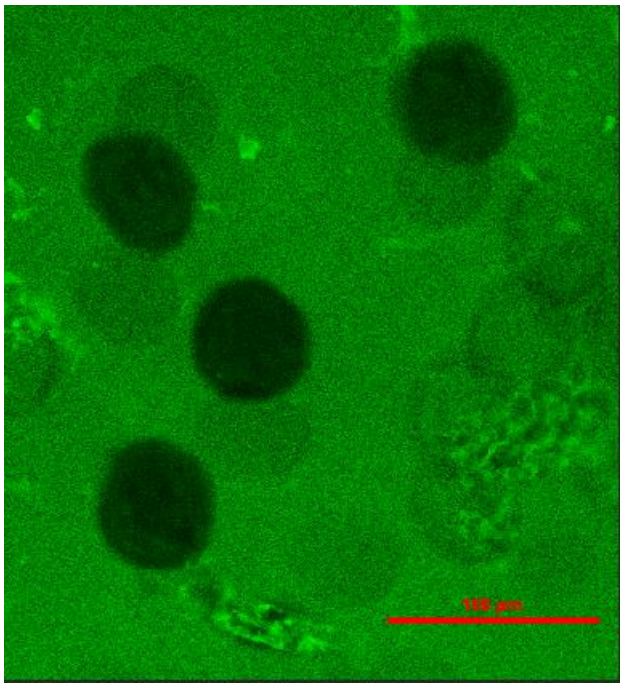

Figura 38 Images of agar-alginate samples from confocal microscopy in black and white (left) and with colour

The penetration depth was calculated by comparing the diameter of the beads before and after being mixed with agarose.
The average diameter after mixing was 64 µm, whereas before mixing was -as previously reported- 66 µm.

The first conclusion that could be drawn is that the radial penetration of agarose is:
(66-64)/2=1µm
As the thickness of cell coating layer is 5 µm, the penetration would not be sufficient to reach the cell inside its microgel: is still true that cells are in contact with the softer microgel.

The second conclusion that could be drawn is that the volume percentage X of the single bead which is penetrated by agarose is negligible (<10% for any size):

$V=4/3\Pi R^3$
$\Delta V=4/3\Pi(R^3-r^3)$
$\Delta V : V = X : 100$

Where X corresponds to:

- X<9% for D=45 µm beads
- X<7% for D=80 µm beads
- X<3% for D=200 µm beads
- X<2% for D=300 µm beads

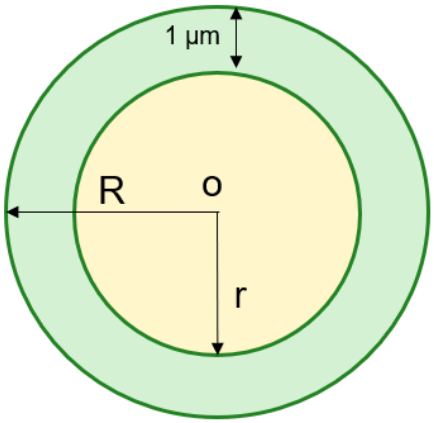

Figura 39 Schematic representation of penetration of agarose inside alginate

2.7 Bibliography

[1] Knee joint forces: prediction, measurement, and significance
Darryl D. D'Lima,[1] Benjamin J. Fregly,[2] Shantanu Patil,[1] Nikolai Steklov,[1] and Clifford W. Colwell, Jr.[1]

[2] Modulation of chondrocyte functions and stiffness-dependent cartilage repair using an injectable enzymatically crosslinked hydrogel with tunable mechanical properties
Li-ShanWang[1]Chanu[1]Wei Seong Toh[2]Andrew C.A.WanShu Jun Gao Motoichi Kurisawa

[3] Single Cell Microgel Based Modular Bioinks for Uncoupled Cellular Micro- and Macroenvironments
Tom Kamperman, Sieger Henke, Albert van den Berg, Su Ryon Shin, Ali Tamayol, Ali Khademhosseini, Marcel Karperien,* and Jeroen Leijten

[4] Directing the assembly of spatially organized multicomponent tissues from the bottom up
Jennifer S.LiuZev J.Gartner

[5] Growth factor binding to the pericellular matrix and its importance in tissue engineering.
Macri L[1], Silverstein D, Clark RA.

[6] Scaffold Translation: Barriers Between Concept and Clinic
Scott J. Hollister, and William L. Murphy

[7] The structure and function of the pericellular matrix of articular cartilage
Rebecca E.WiluszJohannahSanchez-AdamsFarshid Guilak

[8] Hybrid Organic-Inorganic Scaffolding Biomaterials for Regenerative Therapies
Nadege Sachot, Elisabeth Engel, Oscar Castano.

[9] Understanding Rheology of Structured Fluids

[10] Normal force controlled rheology applied to agar gelation
Bosi Mao, Thibaut Divoux, and Patrick Snabrec

[11]In-air microfluidics enables rapid fabrication of emulsions, suspensions, and 3D modular (bio)materials
Claas Willem Visser, Tom Kamperman, Lisanne P. Karbaat, Detlef Lohse, Marcel Karperien

[12] R.-H. Chen, S.-L. Chiu, T.-H. Lin, Collisions of a string of water drops on a water jet of equal diameter. Exp. Therm. Fluid Sci. 31, 75–81 (2006).

[13] S. Wildeman, C. W. Visser, C. Sun, D. Lohse, On the spreading of impacting drops.
J. Fluid Mech. 805, 636–655 (2016).

[14] Mechanical properties of alginate hydrogels manufactured using external gelation
Georgia Kaklamania, David Chenelerd,e, LiamM.Grovera, Michael J.Adamsa, James Bowen

[15] Affinity Purification of Natural Ligands
John H.T. Luong1 and William H. Scouten

Chapter 3

3.1 Abstract

In this section is described how the uncoupling of micro and macroenvironment was pursued by encapsulating cells in two different biomaterials, Dex-TA and PEGDA, where Dex-TA represents the cell micro niche, pericellular matrix (PCM) and PEGDA should be the stiffer ECM.
Since culturing cells on soft Dex-TA and stiff PEGDA would have introduced another variable a part from Elasticity (the biomaterial itself), cells were cultured in contact with both stiff and soft Dex-TA and PEGDA hydrogels.
Specifically, single cell encapsulation in Dex-TA was performed, and half of the obtained microspheres were in turn post cured in order to stiffen the microgel even more, whereas the other half was directly cultured in suspension.
As far as it concerns PEGDA cells were suspended in hydrogel precursor and then crosslinked in order to obtain a stiff or soft bulk scaffold.
Trivially, before preceding to the readout of any chondrogenic marker, is necessary to guarantee cells survival during encapsulation process in both aforesaid biomaterials. Therefore an optimization of encapsulation parameters was necessary.
Cells viability was evaluated and quantified with L/D assay, resulting higher in both soft Dex-TA and PEGDA with respect to the stiffer counterparts.

3.2 Introduction

Hydrogels are nowdays employed as materials in countless biomedical applications, owing to their excellent properties such as biocompatibility, easily tunable properties, bioactivity, high water content and permeability for nutrients and metabolites.
In particular, Dextran was picked to simulate the microniche because is possible to covalently couple the biomaterial directly with cells membrane in a completely independent manner from adesive moieties, as previously reported by Kamperman et al. [1]
In fact biomechanical cues that cells are exposed to, are essential for their survival and function. Cells sense microelasticity by deforming themselves and the pericellular matrix, and respond to these stimuli via mechanotransduction pathways that control migration, proliferation, apoptosis, metabolism, and differentiation.[2, 3] Mechanotransduction is canonically mediated through transmembrane cell adhesion molecules (CAM; e.g. integrins, cadherins, and selectins), and transmitted through the intracellular actinomyosin cytoskeleton (Figure 1).[4]

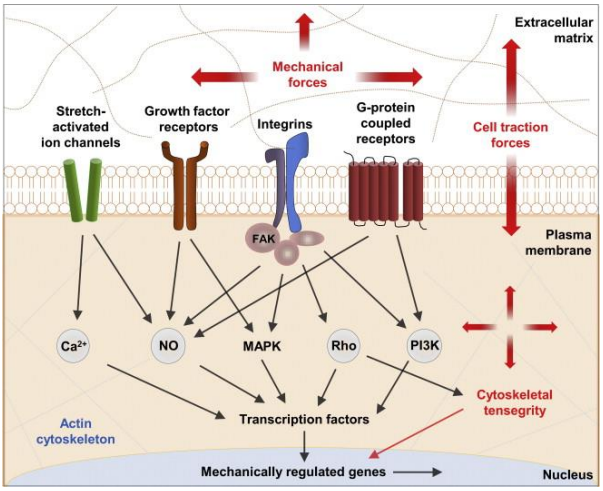

Figure 10 Mechanotransduction through CAMs

To reproduce these biological events in engineered tissues, biomaterials have typically been endowed with cell adhesive moieties that specifically bind to these CAMs. In particular, the integrin binding tripeptide arginine-glycine-aspartic acid (RGD) has been widely explored to this end.[5]
Although enzymatic crosslinking has been harnessed to endow native tissues and biomaterials with biofunctional moieties such as RGD-type peptides,[6, 7] now it will be adopted as approach to directly tether a non adesive biomaterial directly onto cells.
In order to reach this goal the Dextran was functionalized as previously reported [8] with Tyramine, which is a naturally occurring phenolic trace amine.
It was adopted a highly specific enzymatic crosslinking mechanism based on Tyrosine-Tyramine coupling, which is known to stabilize proteins in native tissues.[9] Tyrosines are abundantly present in the extracellular domains of transmembrane proteins[10] and can be coupled to other phenolic moieties -like Tyramine- using a cytocompatible enzymatic crosslinking reaction.[11]
In fact, Tyramine and Tyrosine units can be covalently bound by leveraging an enzyme called Horse Radish Peroxidase (HRP) which catalyzes the coupling of phenolic groups in presence of Hydrogen Peroxidase as an oxidiser (Figure 1).
By leveraging such a chemical mechanism, it was possible to obtain on-a-chip single cell laden microgels whose viability was evaluated overtime.

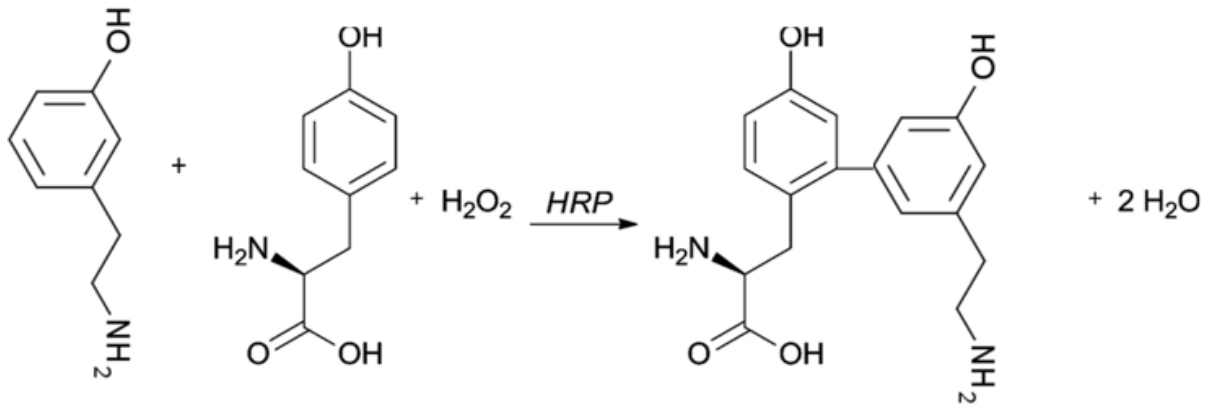

Figure 11 Chemical reaction between Tyramine and Tyrosine with HRP and Hydrogen Peroxidase

As far as it concerns cell encapsulation in PEGDA, a traditional approach with UV crosslinking was adopted, and cells were encapsulated in a bulk scaffold instead of into a single cell laden microgel. With this method, the UV light induced the crosslinking of PEGDA polymer chains in presence of a photoinitiator, Irgacure 2959 (figure1)

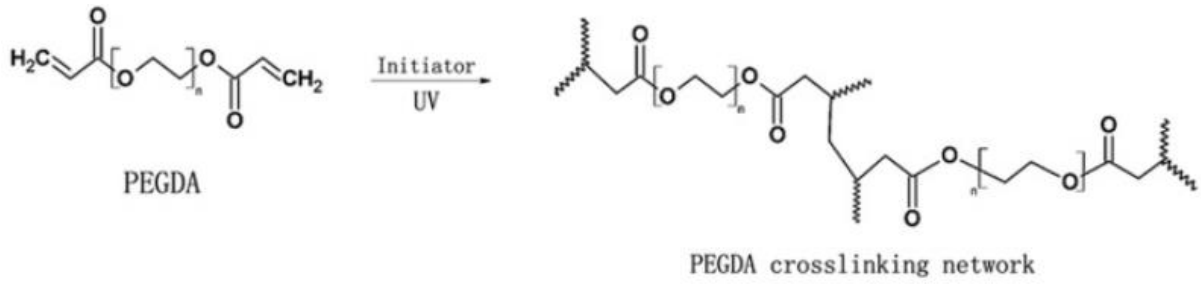

Figure 12 Crosslinking mechanism of PEGDA in presence of I2959 through UV irradiation

Soft and stiff PEGDA were obtained tuning the polymer concentration in hydrogel precursor solution, and their effects over cells viability were evaluated.

3.3 Materials

Dextran (MW 35-45 kg/mol) was functionalized with tyramine, as previously described.[12] The resulting dextran-tyramine (Dex-TA) contained ~10 tyramine moieties per 100 repetitive monosaccharide units. Horseradish peroxidase (HRP, type VI), hydrogen peroxide (H_2O_2; with inhibitor), tyramine, tyrosine, fetal bovine serum (FBS), ascorbic acid, iodixanol (OptiPrep), insulin (human), dexamethasone, Calcein AM, ethidium homodimer-1 (EthD-1), Oil Red O, Alizarin Red S, and all other solvents were purchased from Sigma-Aldrich. Cell strainers were purchased from Corning.

Phosphate-buffered saline (PBS) was purchased from Lonza. Minimal Essential Medium α with nucleosides (αMEM), Penicillin and Streptomycin, GlutaMAX, and trypsin-EDTA were purchased from Gibco.

Catalase (from bovine liver) was purchased from Wako. Polydimethylsiloxane (PDMS, Sylgard 184) was purchased from Dow Corning. Aquapel was purchased from Vulcavite. Pico-Surf 1 in Novec 7500 Engineered Fluid and Pico-Break 1 were purchased from Dolomite. Surfactant-free fluorocarbon oil (Novec 7500 Engineered Fluid) was kindly provided by the BIOS Lab-on-a-Chip group. Gastight syringes (Hamilton), fluorinated ethylene propylene tubing (FEP, inner diameter 250 µm, DuPont) and connectors were purchased from IDEX Health and Science. Low pressure syringe pumps (neMESYS) were purchased from Cetoni.

3.4Methods

3.4.1 Cells thawing

A vial of bovine chondrocytes (1ml; 10^6 cells/ml) was thawed from a liquid nitrogen container (T=-180°C).
First of all, the frozen vial was placed into a water bath (T=37°C) until a last lump of ice was present. Then, the content of the vial was poured into a 50ml sterile plastic tube and a first ml of cell proliferation medium (consisting of 10% FBS, 100U/ml Penycillin, 100µg/ml Streptomycin, 0.2mM ascorbic acid, 1% GlutaMax in DMEM) was added drop by drop. Afterwards 3 further ml of medium were added and the cells resuspended by pipetting up and down.
Subsequently the tube with its content was centrifuged at 300g for 180s; afterwards the supernatant was aspirated in order to remove the DMSO present in the initial vial. Then new medium was added and cells were resuspended and counted. As last step cells were transferred into a 175 cm^2 flask to be cultured with a density of 3500 cells per cm^2.
The procedure is illustrated in Figure 4.

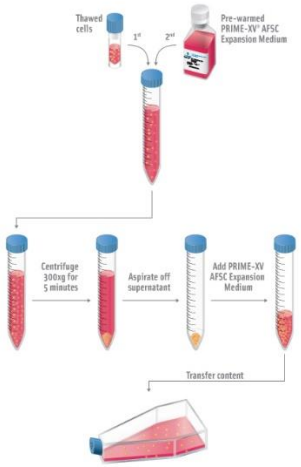

Figure 13 Thawing cells protocol

3.4.2 Cells culture

After being transferred into the flask, the culture medium was changed twice a week.
When confluence was reached, cells were subcultured and transferred into a new flask in order to maintain a proper density during cell culture. The protocol used during subculture is reported.
Briefly, when confluence was reached, culture medium was removed with an aspirator and cells were washed with PBS solution.
Then, PBS was aspirated and 2-3 ml of Trypsin-EDTA were pipetted directly onto cells. The flask was tightly closed and tilted in order to let the Trypsin-EDTA spread all over the flask surface and placed into an incubator (T=35°C, CO_2=5%) for 1-3min.
Afterwards the cells were no longer attached to the flask, but suspended in the Trypsin-EDTA solution. Such solution was then neutralized by pipetting 7-8 ml of proliferation medium; the content was pipetted up and down with a 10ml serological pipet in order to unravel cells lumps. Everything was transferred into a 10/50ml plastic tube and centrifuged as above.
The next step was removing the supernatant were Trypsin-EDTA was still present and adding new fresh medium. Cells were resuspended, counted and transferred into a new flask(s).

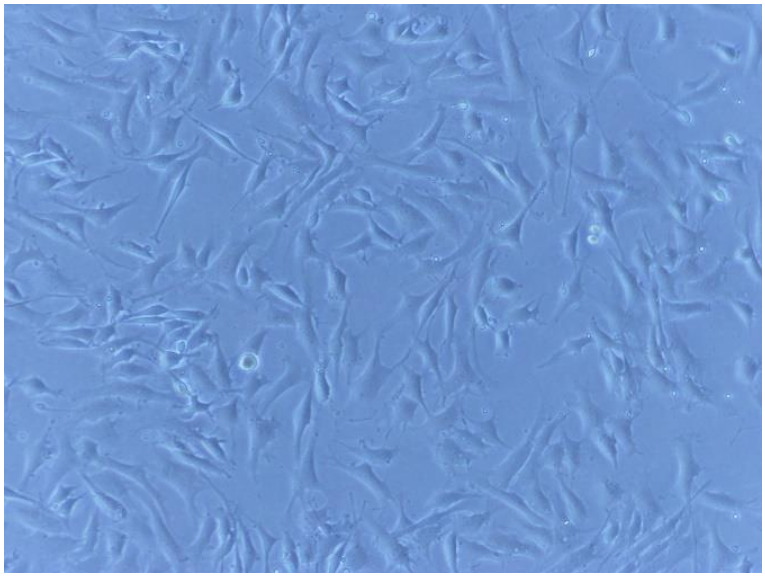

Figure 14 Chondrocytes proliferation (confluence approx. 60%)

3.4.3 Cells encapsulation

Since in the long period cells tend to become senescent, encapsulation was always performed at passage<5.
Right below is reported the procedure followed for encapsulation in both Dex-TA and PEGDA.

3.4.3.1 Dex-TA encapsulation

3.4.3.1.1 Hyrdogel precursor

To produce cell laden microgels, detached cells (passage 1 to 5) were washed with medium, flown through a 40 µm cell strainer, and suspended in the hydrogel precursor solution at a concentration of 10^7 cells per ml.
Hydrogel precursor solution contained 10% Dex-TA dissolved in culture medium, 44U/ml HRP, 8% OptiPrep (i.e. to obtain 1.05 g/ml density) and cells laden culture medium.
In order to assess the cytocompatibility of the hydrogel precursor, an aliquot was withdrawn and a L/D assay was performed, Figure 6.

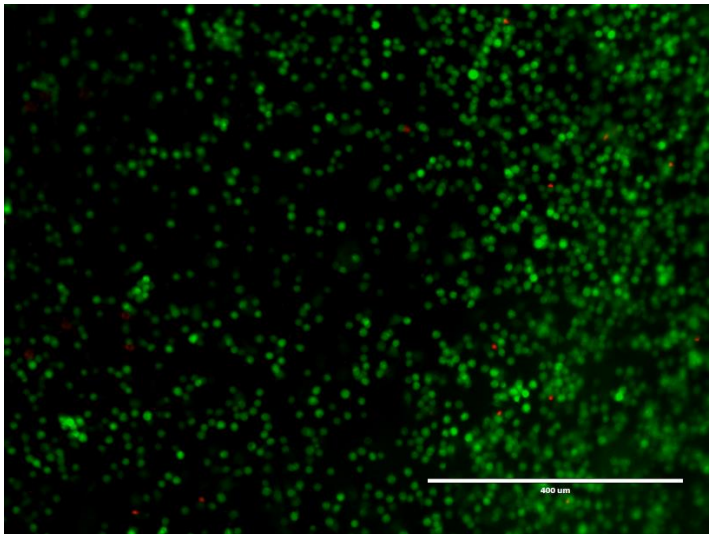

Figure 15 Cell viability in hydrogel precursor: 99,7% L

3.4.3.1.2 Encapsulation platform

Cell laden microgels were produced by emulsifying the hydrophilic hydrogel precursor micro droplets into a second immiscible oil phase through a microfluidic flow focusing device.
The platform consisted of a syringe 'low pressure' pump where syringes with hydrogel precursor, oil and Hydrogen Peroxide were placed.
Such syringes were linked, through opportune plastic connectors, to FEP tubing where their content could flow and reach the first PDMS chip: a micro-droplet generator. FEP tubing was also used to connect the first chip to the second one: a H_2O_2 diffusion-based crosslinking channel. The outlet of the second chip was linked -always through FEP tubing- to a 1.5ml Eppendorf tube where cell laden microgels were collected.
The components of the aforesaid platform are described in detail right below.

3.4.3.1.2.1 Syringe pump

Four syringes were placed onto the pump (which was controlled via computer): one with cell laden hydrogel precursor, two with oil (2% PicoSurf 1 containing 7500 Novec Engineered Fluid) and a last syringe containing Hydrogen Peroxide solution.
The flow rates used to actuate the syringes were 1.5µl/min and 6 µl/min for hydrogel precursor and oil respectively (1:4 ratio), and 30µl/min for Hydrogen peroxide.
All the syringes were ice-cooled during the whole process in order to optimize the flow and guarantee an optimal viscosity.
Furthermore, the hydrogel precursor was gently agitated every 10min through a stirring bar and a tiny spherical magnet placed into the syringe in order to prevent cells from precipitating to the bottom.

Figure 16 Chetoni Nemesys 'low pressure' pump. The flow rates were set from Nemesys software

3.4.3.1.2.2 PDMS chips

Both the PDMS chips were manufactured from a silica wafer through standard soft lithography techniques. Afterwards, PDMS was gently detached from the wafer and chips were cut out with a sterile blade. Subsequently chips were opportunely punched in order to create inlets and outlets. Afterwards were covalently fixed onto microscope glass slides thanks to the activation of reactive groups into a plasma oven.
Before usage, Aquapel was introduced in the chips to ensure channel wall hydrophobicity.

3.4.3.1.2.2.1 Droplet generator

Such chip was fabricated with ~25µm high channels. From the central one, the cell laden hydrogel precursor was injected, whereas from the side channels oil was provided. The emulsified micro droplets could flow through the outlet channel, where FEP tubing allowed them to flow to the second chip.

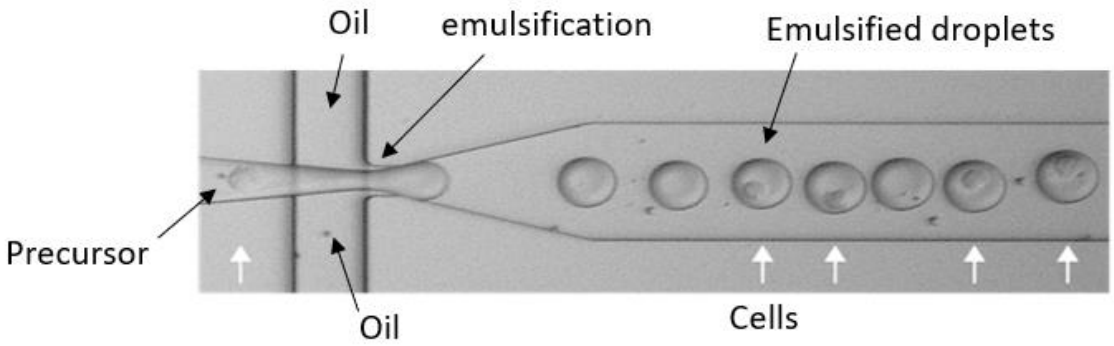

Figure 17 Micro droplet generator

3.4.3.1.2.2.2 Crosslinking channel

The second chip was fabricated with ~100 µm high channels.
Three parallel channels are present: two side ones where H_2O_2 flows, and a central channel where emulsified droplets are crosslinked thanks to the diffusion of H_2O_2 through PDMS, Figure 9.
The thickness of PDMS wall which divides the crosslinking channel from the ones where Hydrogen Peroxide flows is ~50 µm. The total length of the channels is 35cm, enough to allow the complete crosslinking of the precursor emulsified droplets which were subsequently collected into a 1,5ml Eppendorf tube.

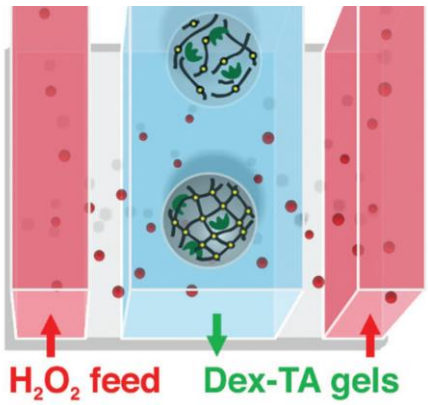

Figure 18 Crosslinking channel chip (Advanced Healthcare Materials, 2016)

3.4.3.1.3 Emulsion breaking

Once the encapsulation was complete, the emulsion in oil was broken by washing three times with surfactant free fluorocarbon oil and subsequent supplementation of Pico Break 1 in the presence of PBS or serum containing proliferation medium. Retrieved cell laden microgels were cultured in proliferation medium.

3.4.3.1.4 Microgel post curing

Half of the produced microgels were then post cured in order to stiffen the cells' substrate and evaluate the cell viability onto stiffer Dex-TA.
The protocol which was used is reported.

- Microgels were put into a 14ml plastic tube
- Centrifuged at 300g, 120s
- Supernatant was removed
- Were added 1ml cell proliferation medium + 100µl 850U/ml HRP
- The tube was incubated 15-30min
- 1ml 0,06% H_2O_2 was added and the solution pipetted up and down
- After 60-90s, 1ml of catalase solution was added (1ml medium + 25µl 10^6U/ml catalase) and the solution pipetted up and down
- The tube was centrifuged as above
- The supernatant was removed and the microgels washed 1x with medium
- Microgels were placed in 6well plate and cultured

3.4.3.2 PEGDA encapsulation

3.4.3.2.1 Hydrogel precursor

To produce cell laden hydrogel bulk, detached cells (passage 1 to 5) were washed with medium, flown through a 40 µm cell strainer, and suspended in the hydrogel precursor solution at a concentration of 10^7 cells per ml.
Hydrogel precursor solution contained either 25% w/v PEGDA 3400 g/mol (to obtain stiff PEGDA) or 15% w/v PEGDA 3400 g/mol (to obtain soft PEGDA) in proliferation medium. In both cases the solution also contained 0.05% I2959 as a photoinitiator.
Before of inducing gelation, an aliquot was withdrawn from both the precursors in order to ensure the solutions not to be cytotoxic.
The L/D assay is reported right below, Figure 10-11.

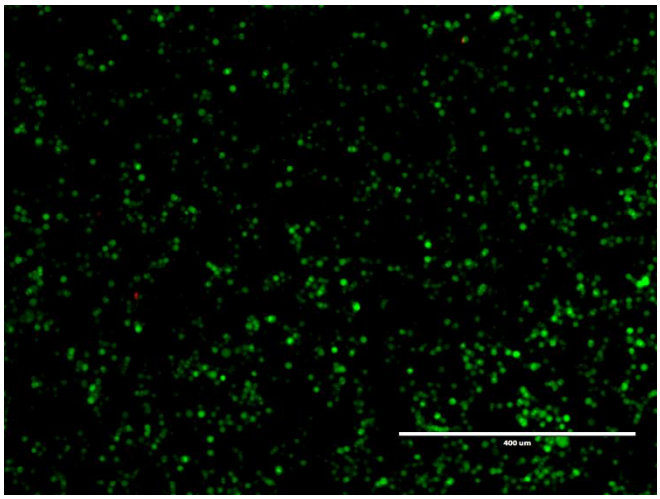

Figure 19 L/D on 15% PEGDA hydrogel precursor. L=99,9%

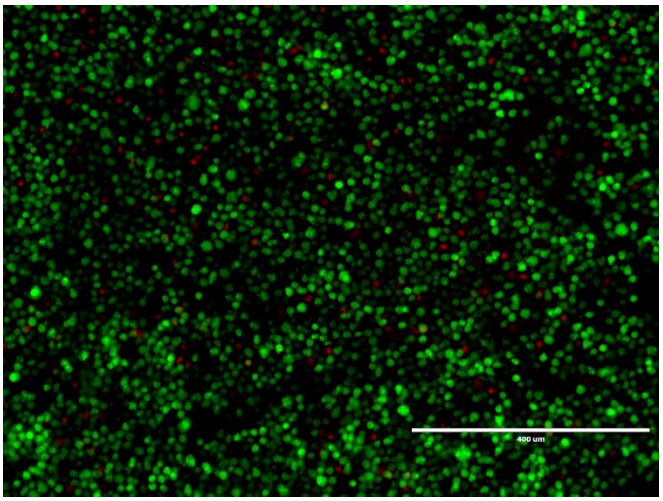

Figure 20 L/D on 25% PEGDA hydrogel precursor. L=96,4%

3.4.3.2.2 Encapsulation method

Every sample consisted of 130 µL of the cell/PEGDA solution which was added to sterilized molds created from the detached caps of 1.5 ml polypropylene centrifuge tubes. The final construct had a thickness of approximately 2mm and 9mm as a diameter.
The molds with hydrogel precursor were placed under a UV light source (Hamamatsu LC8, 365nm; Figure 12) which induced the precursor gelation.
Afterwards, the disks were removed from the molds and immediately put into proliferation medium, where cell viability was evaluated overtime.

Figure 21 Hamamatsu LC8, λ=365nm

3.5 Results and discussion

3.5.1 Dex-TA

Cell laden microgels were produced.

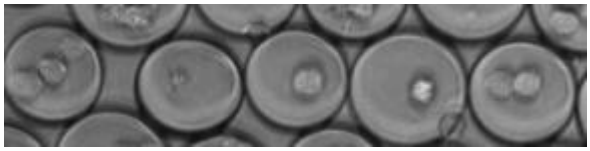

Figure 22 Cell laden Dex-TA microgels

The most critical parameter during the whole procedure was the concentration of Hydrogen Peroxide solution: in fact, in case of too low concentration gelation would have been incomplete, whereas an excessive concentration would result cytotoxic [].
The critical concentration inducing cytotoxicity depends on some parameters of the polymer, i.e. molecular weight (MW) and the degree of substitution of Tyramine moieties in Dextran chains (DS).
In this experiment several H_2O_2 concentration were tested: 1-2-3-5% w/v respectively and the results were compared with the ones obtained by Kamperman et al., where the same material was used with a different MW and DS.

First of all, cell viability was evaluated (Figure 13-16) and quantified (Figure 17) immediately after encapsulation.

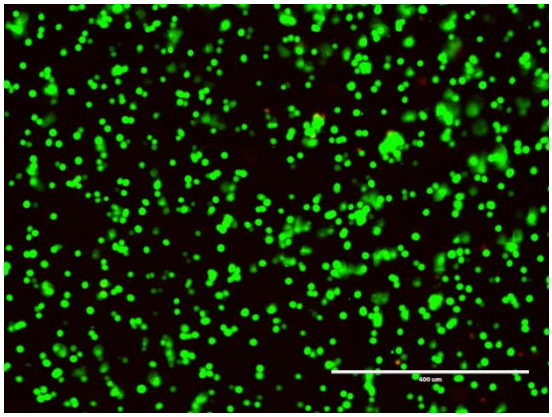

Figure 23 L/D assay with Hydrogen Peroxide concentration 1%

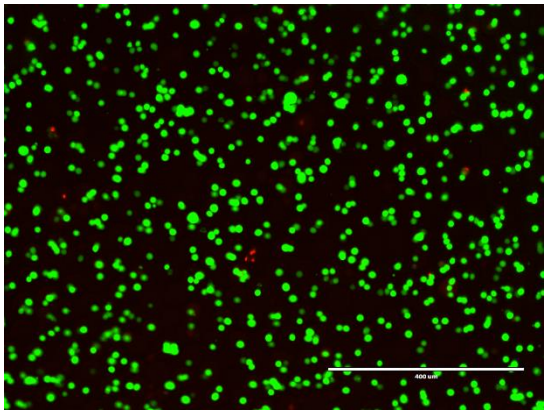

Figure 15 L/D assay with Hydrogen Peroxide concentration 2%

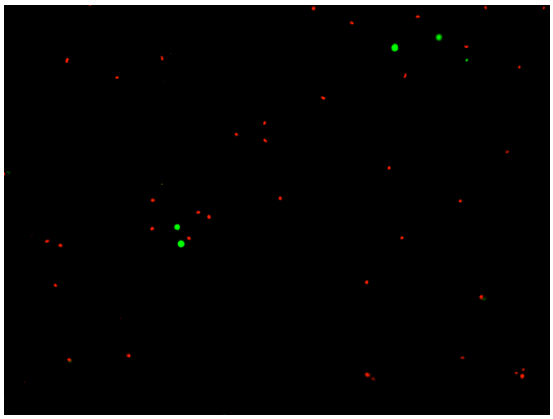

Figure 16 L/D assay with Hydrogen Peroxide concentration 3%

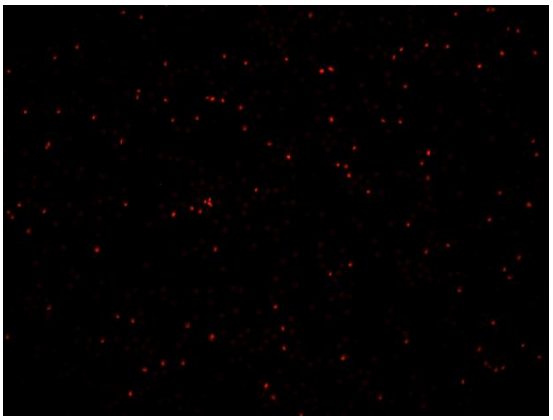

Figure 17 L/D assay with Hydrogen Peroxide concentration 5%

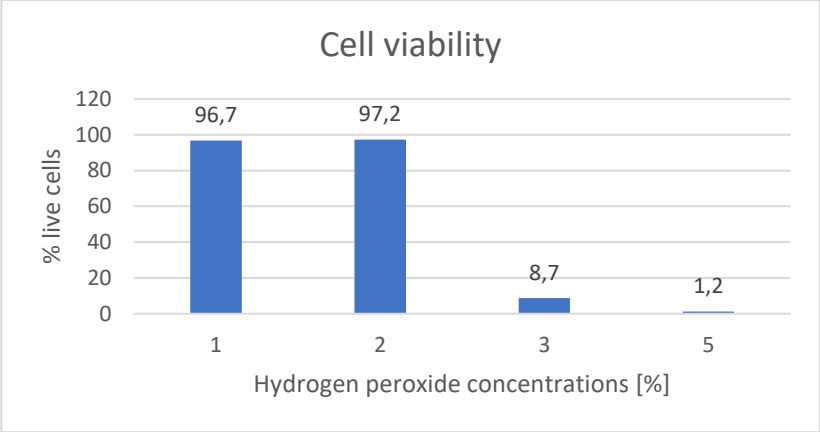

Figure 18 Cell viability at D0 for all the concentrations

As reported in the pictures, the only concentrations able to guarantee cells survival to encapsulation process resulted to be 1-2% H_2O_2. For this reason, the following results will only concern cells encapsulated with these two concentrations.

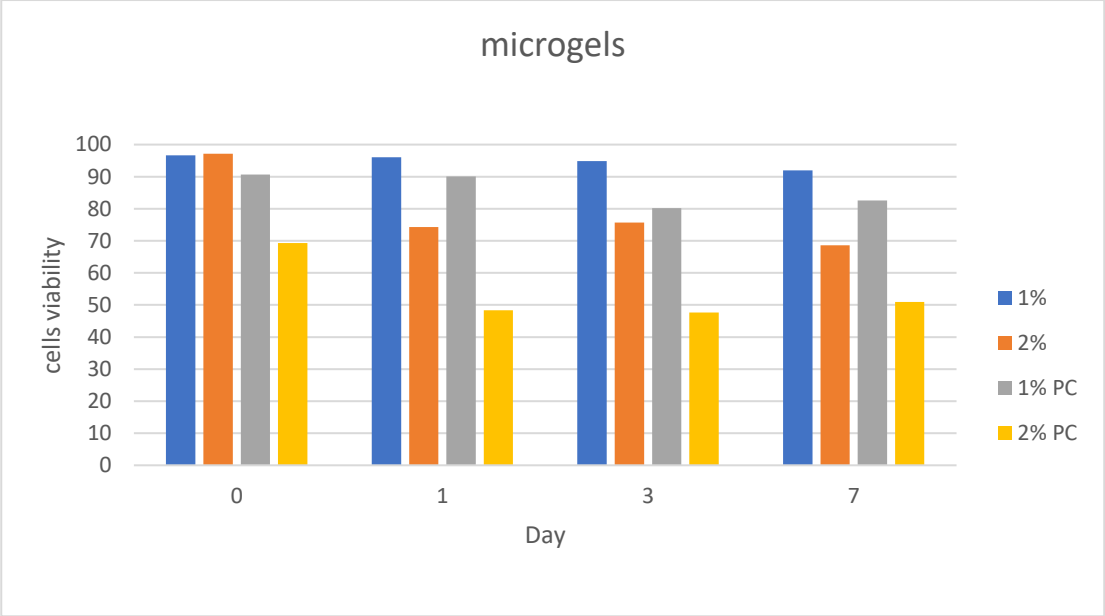

Figure 19 Cell viability overtime in microgels and post cured microgels

As previously mentioned, after microgels production 50% of both 1% and 2% batches were post cured (PC) to make them stiffer, whereas the remaining 50% was immediately put into culture without any further treatment.
The cells viability was evaluated and quantified overtime.

First of all, is possible to immediately notice that after D0 cells encapsulated with a H_2O_2 concentration of 2% reduced their viability. Most likely the reason is that even if such a concentration didn't kill cells during encapsulation, it was a borderline situation: cells didn't die, but even so were highly stressed. This could induce apoptosis a few hours after microgels production.
A fact which seems to confirm this hypothesis is that after post curing -always at D0- approx. 20% of cells died after being exposed to a further dose of HRP and H_2O_2: cells didn't recover from the stress due to encapsulation with 2% H_2O_2 and then couldn't bear post curing.
Furthermore, cells encapsulated with 1% H_2O_2 were exposed to the same dose of HRP and Hydrogen Peroxide during post curing, but the decrease of cell viability was minimum (blue grey bars). Therefore is logic to attribute the difference in cell viability to the only parameter which was tuned during the experiment: the H_2O_2 concentration during hydrogel precursor crosslinking.
Also, the mechanical properties of all the hydrogels (1%, 1% PC, 2%, 2% PC) were evaluated through rheology as described in chapter 2 and reported right below.

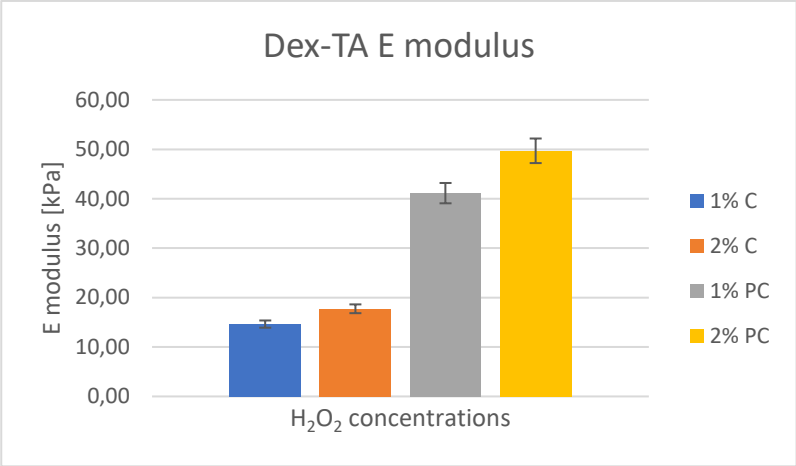

Figure 20 Mechanical properties of Dex-TA used in cell encapsulation

What can be immediately noticed is that the E modulus of not post cured microgels is optimal for chondrogenesis, whereas the elasticity of post cured microgels (~ 40-50 kPa) is associated to osteogenesis [1].
Even so, such an elasticity is absolutely compatible with cell survival, and reasonably the lower cell viability in both non and post cured microgels with 2% H_2O_2 is not due to the mechanical properties of the hydrogel (notably, cells viability is higher in post cured 1% microgels than in NOT post cured 2% ones).

The results were compared with the ones from previous experiments (Figure 20-21) [14] where the same cell type and biomaterial were used, but the latter with a different MW and DS.
In particular, 15-25kg/mol vs 35-45kg/mol and 15% vs 10% as a DS for previous experiments and the ones presented above respectively.

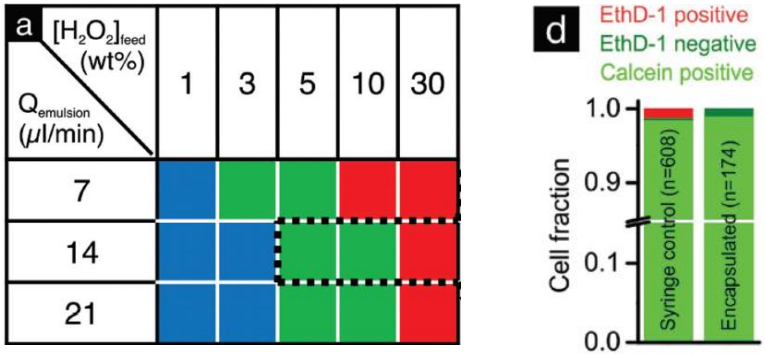

Figure 21 Optimal Hydrogen Peroxide concentration and relative cells viability (Kamperman et al. 2017)

It is possible to notice that with an almost identical emulsion flow rate (7 vs 6µl/min) and a H_2O_2 concentration of 5%, cell viability was ~100% vs 1,2%.
The hypothesis formulated to explain such a difference is the higher gelation time and the higher degree of substitution of the polymer used in Kamperman's experiments.

As far as it concerns gelation time, it decreases when the molecular weight of the polymer increases [15]. For this reason, the polymer with higher molecular weight could have reached complete gelation already in the first half of the length of crosslinking channel.
This means that during the transit of the cell laden microgel in the final part of the channel, Hydrogen Peroxide has acted directly onto cells and damaging cell membrane, instead of acting on the polymer which was already completely crosslinked.
As far as it concerns the degree of substitution, is intuitive that if a polymer chain presents more crosslinking moieties, H_2O_2 will act on such chemical groups rather than on cell.
So, a lower degree of substitution -keeping constant the H_2O_2 concentration during encapsulation- could cause a decrease in cells viability and vice versa.
The relationship between all the aforesaid parameters is reported in the table below.

	Gelation time	Critical H_2O_2 concentration
Molecular weight ↑	↓	↓
Degree of substitution ↑	↓	↑

3.5.2 PEGDA

The most critical parameters during the encapsulation process were the UV light intensity and the exposure time. In fact the values which were previously reported in literature by Mozzoccoli et al. [16] resulted to be cytotoxic and damaging for cells; then it was necessary to optimize them in order to guarantee both short and long term cells survival.

3.5.2.1 Hydrogel precursor and polymer characterization

Likewise it was done for Dex-TA, first of all the cytocompatibility of the hydrogel precursor was evaluated with several polymer concentration and molecular weights (MW). In particular, 15% and 25% w/v were the concentrations used to obtain soft and stiff PEGDA respectively. As far as it concerns the MW, 575 and 3400 g/mol PEGDA were used.
The first step was quantifying the mechanical properties (i.e. Elastic modulus) of the hydrogels.

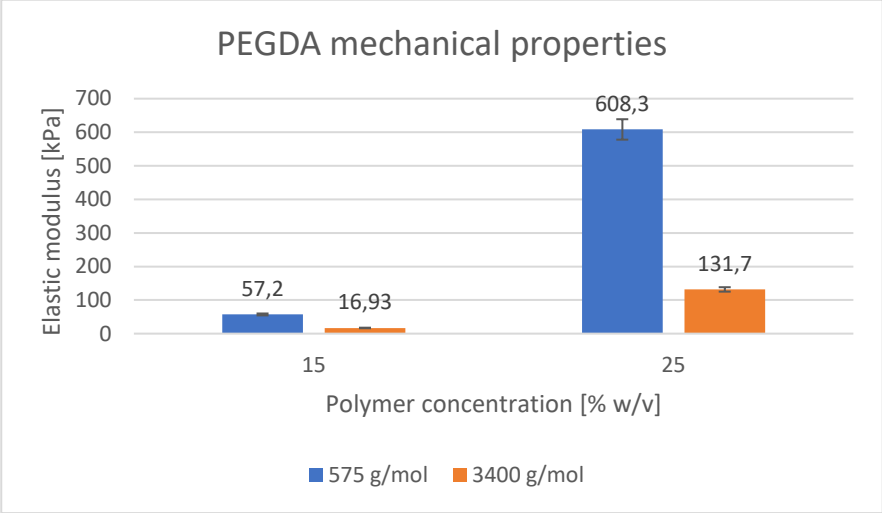

Figure 22 PEGDA mechanical properties as a function of MW and concentration

As expected, the E modulus was higher for the polymer with lower MW.
In particular, at 15% w/v, PEGDA 3400 tested to perfectly fit the range of elasticity to enhance chondrogenesis (10-20 kPa).

The L/D assays was then performed on all the combinations.

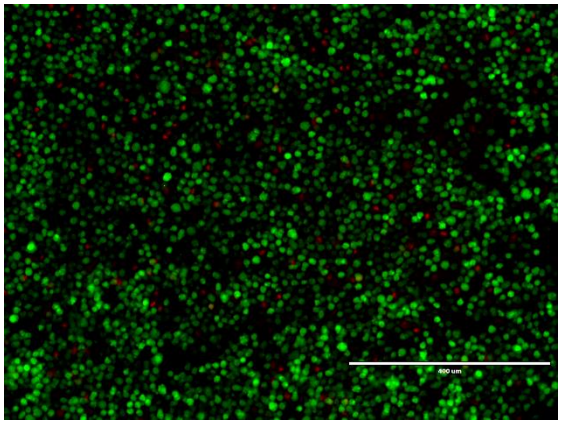

Figure 23 L/D assay PEGDA 575g/mol at 15%w/v. L=97,9%

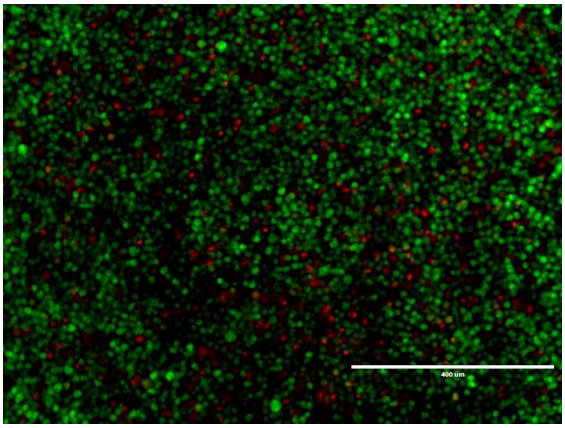

Figure 24 L/D assay PEGDA 575 g/mol at 25% w/v. L=93,8.

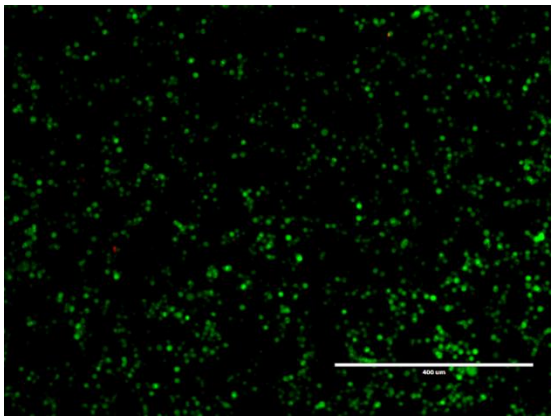

Figure 25 L/D assay PEGDA 3400 g/mol at 15% w/v. L=100%

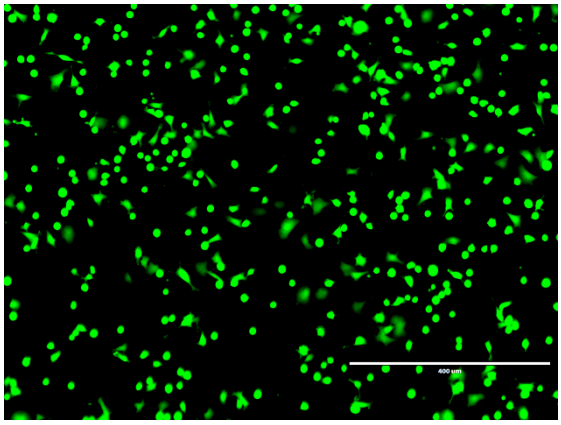

Figure 26 L/D assay PEGDA 3400 g/mol at 25% w/v. L=100%

First of all, cells viability was higher than 90% for all the combinations, but even higher when MW of the polymer was higher. The reason is that Diacrylate groups at the beginning and the end of PEG chains are not very safe for cells and when the MW decreases- keeping constant the w/v percentage- the number of polymer chains in the solution increase, as well as the number of Diacrylate groups.
As a consequence, a higher number of Diacrylate groups means a higher production of free radicals during exposure to UV light, which is detrimental for cells.

3.5.2.2 Encapsulation

Several exposure times [s] and UV intensity [mW/cm^2] were tested.
The trend which was noticed is that, keeping constant the amount of energy per cm^2 [J/cm^2=s*mW/cm^2], was much safer for cells being exposed to lower UV intensity for longer periods rather than the opposite.
Right below is reported the L/D assay performed onto the cell laden PEGDA scaffold at D0 - immediately after being encapsulated- using the same amount of energy but different exposure times and UV intensity.

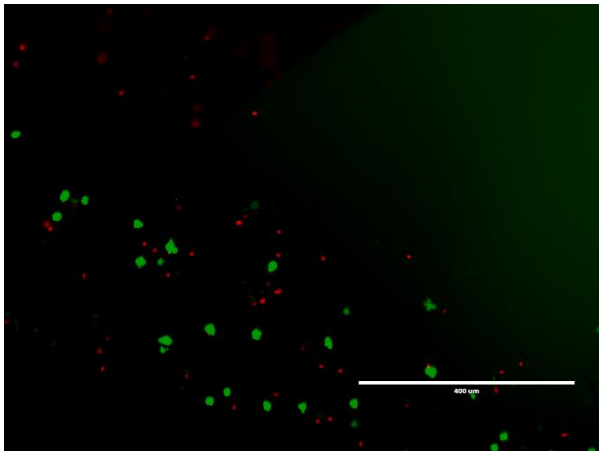

Figure 27 L/D assay PEGDA 15% w/v after 96s at 50mW/cm^2 L=49%, D0

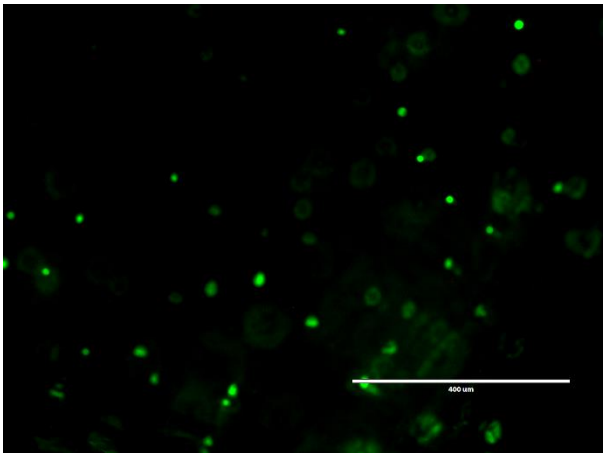

Figure 28 L/D assay PEGDA 15% w/v after 600s at 8mW/cm^2 L=73%

Is possible to immediately notice that a lower UV intensity is safer as the amount of live cells is higher. But what is even more remarkable are the effects at D1.

Firstly, only the results relative to PEGDA 3400g/mol are reported, since cells in PEGDA with lower MW were all dead for any UV light intensity and exposure time, most likely because of the excess of free radicals produced during encapsulation, as previously mentioned.

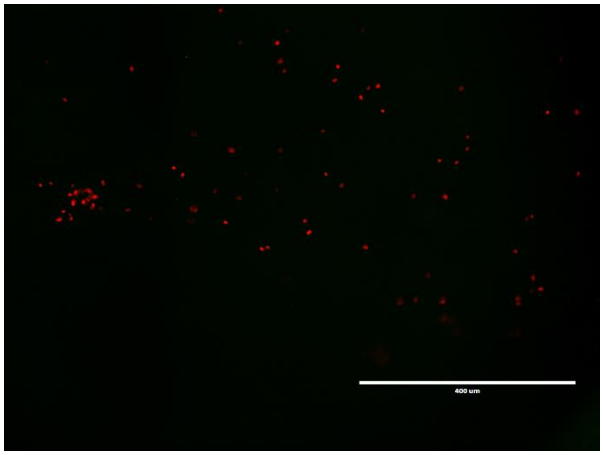

Figure 29 L/D assay PEGDA 15% w/v after 96s at 50mW/cm^2 L=0%, D1

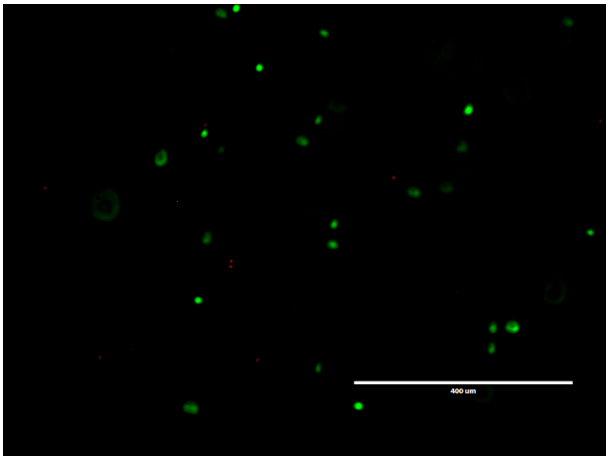

Figure 30 L/D assay PEGDA 15% w/v after 600s at 8mW/cm^2 L=82,4%, D1

The reason why cells in the left picture die after D0 is that the effects of free radicals produced during encapsulation procedure are not exactly immediate, in fact could also take several hours (i.e. 12-24h); whereas as far as it concerns the right picture, the lower UV intensity allows a lower production of radicals, and cells viability at D1 is higher than D0 because they were not damaged during encapsulation, so it was possible to start proliferating and increase in this way the percentage of live cells.
Their viability was evaluated overtime and the trend is reported right below.

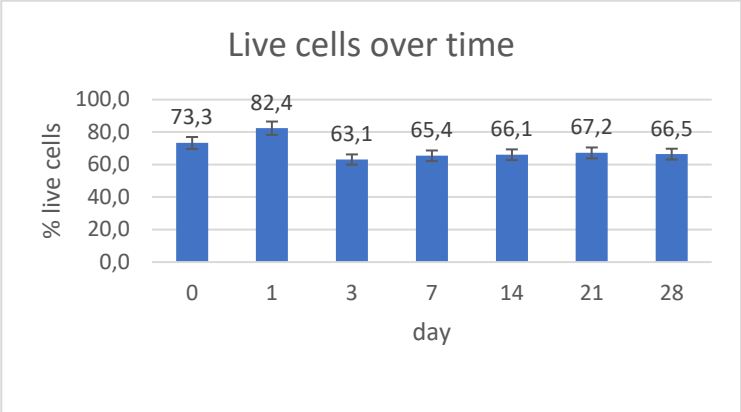

Figure 31 Cells viability overtime in PEGDA 3400 g/mol 15% w/v

Is possible to immediately observe that between D1 and D3 there was a decrease of live cells, whereas after D3 cells viability was extremely stable overtime, confirming that the encapsulation process was indeed cytocompatible.

As it was made with Dex-TA, also a stiffer PEGDA was tested in order to investigate the effects of the stiffness on cell viability.

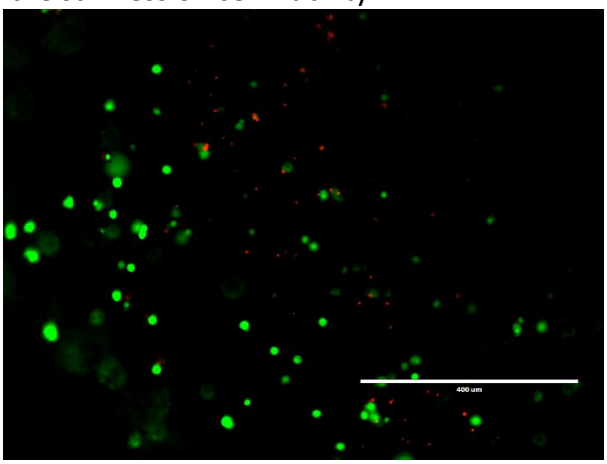

Figure 32 L/D assay PEGDA 3400 g/mol 25% w/v; L=69,3%

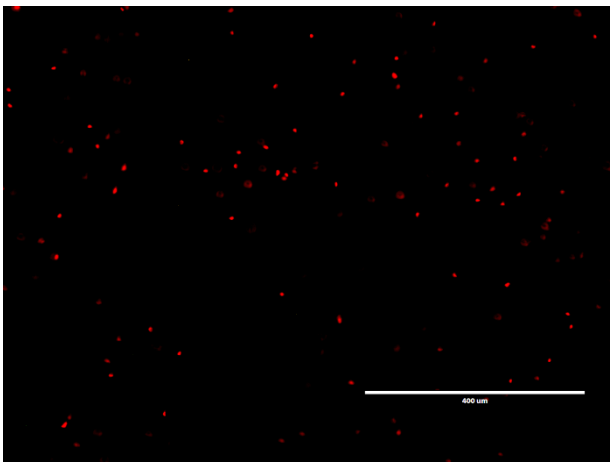

Figure 33 L/D assay PEGDA 3400 g/mol 25% w/v; L=0% ca

At D0, immediately after encapsulation, the percentage of live cells was comparable with PEGDA 15% w/v, but ad D1 all cells resulted to be dead.
Now, the production of free radicals during encapsulation process is comparable: same length of polymer chains, and the number of chains itself in the hydrogel precursor was comparable as well:

25/15=1,66 times higher, not enough to justify the death of all cells.
The conclusion which was possible to draw is that the Elasticity of 25% w/v PEGDA was not compatible with survival of chondrocytes, inducing apoptosis 24h after being encapsulated.
Right below is reported a table which summarizes the result and the reasons of cells death during or after encapsulation.

PEGDA	15% w/v	25% w/v
575 g/mol	Cells death; cause: excess of free radicals	Cells death; cause: excess of free radicals
3400 g/mol	Cells survival; restrained production of free radicals, and optimal elasticity of the substrate	Cells death; cause: excessive elasticity modulus of the substrate

3.6 Future work

Once that cell encapsulation was optimized, those who will take over the project will need to perform the following steps:

- Place cell laden Dex-TA microgels into a stiff PEGDA bulk (i.e. 3400 g/mol, 25% w/v): as cells are coated with something soft (E=~20kPa) are not expected to be influenced by the stiffer macro environment.
- Assess cartilage ECM production overtime through opportune markers (e.g. Col II, Col VI, Aggrecans etc.)

3.7 Bibliography

[1] Microgel Technology to Advance Modular Tissue Engineering
T. Kamperman

[2] Tissue cells feel and respond to the stiffness of their substrate. Science, 2005. 310(5751): p. 1139-43. *Discher, D.E., P. Janmey, and Y.L. Wang*

[3] Harnessing traction-mediated manipulation of the cell/matrix interface to control stem-cell fate. Nat Mater, 2010. 9(6): p. 518-26.
Huebsch, N., et al.,

[4] Mechanotransduction and extracellular matrix homeostasis. Nat Rev Mol Cell Biol, 2014. 15(12): p. 802-12.
Humphrey, J.D., E.R. Dufresne, and M.A. Schwartz,

[5] RGD modified polymers: biomaterials for stimulated cell adhesion and beyond. Biomaterials, 2003. 24(24): p. 4385-415.
Hersel, U., C. Dahmen, and H. Kessler

[6] Biomolecular hydrogels formed and degraded via site-specific enzymatic reactions. Biomacromolecules, 2007. 8(10): p. 3000-7.
Ehrbar, M., et al.

[7] Facile coupling of synthetic peptides and peptide-polymer conjugates to cartilage via transglutaminase enzyme. Biomaterials, 2007. 28(35): p. 5215-24.
Jones, M.E. and P.B. Messersmith,

[8] Horseradish peroxidase (HRP) as a tool in green chemistry
Guido R. Lopes, Diana C. G. A. Pinto and Artur M. S. Silva

[9] The chemistry of natural enzyme-induced cross-links of proteins. Amino Acids, 1991. 1(3): p. 293-306.
Bailey, A.J.

[10] Comprehensive analysis of the numbers, lengths and amino acid compositions of transmembrane helices in prokaryotic, eukaryotic and viral integral membrane proteins of high-resolution structure. J Biomol Struct Dyn, 2017: p. 1-22.
Saidijam, M., S. Azizpour, and S.G. Patching,

[11] Dityrosine Cross-Linking in Designing Biomaterials. ACS Biomaterials Science & Engineering, 2016. 2(12): p. 2108-2121.
Partlow, B.P., et al.

[12] Monodisperse collagen gelatin beads as potential platforms for 3D cell culturing. Journal of Materials Chemistry B, 2013. (38): p. 5128
Ma, S., et al.

[13] Apoptosis induced by hydrogen peroxide is mediated by decreased superoxide anion concentration and reduction of intracellular milieu
Clement et al. 1998

[14] Centering Single Cells in Microgels via Delayed Crosslinking Supports Long-Term 3D Culture by Preventing Cell Escape
Kamperman et al. 2017

[15] Injectable hydrogels for cartilage tissue engineering
R.Jin et al. 2009

[16] Mechanical and Cell Viability Properties of Crosslinked Low and High Molecular Weight Poly(ethylene glycol) Diacrylate Blends
Mazzoccoli et al.

3.8 Acknowledgments

Prof. Chiara Tonda-Turo, DIMEAS, PoliTo
Prof. Jeroen C.H. Leijten, DBE, University of Twente
Dr Tom Kamperman, DBE, University of Twente
Dr Jacqueline Plass, DBE, University of Twente
Dr Bram Zoetebier, DBE, University of Twente